© 2014. Published by The Company of Biologists Ltd | Development (2014) 141, 1342-1353 doi:10.1242/dev.102434

RESEARCH ARTICLE

MIG-10 (lamellipodin) has netrin-independent functions and is a FOS-1A transcriptional target during anchor cell invasion in *C. elegans*

Zheng Wang, Qiuyi Chi and David R. Sherwood*

ABSTRACT

To transmigrate basement membrane, cells must coordinate distinct signaling activities to breach and pass through this dense extracellular matrix barrier. Netrin expression and activity are strongly associated with invasion in developmental and pathological processes, but how netrin signaling is coordinated with other pathways during invasion is poorly understood. Using the model of anchor cell (AC) invasion in *C. elegans*, we have previously shown that the integrin receptor heterodimer INA-1/PAT-3 promotes netrin receptor UNC-40 (DCC) localization to the invasive cell membrane of the AC. UNC-6 (netrin)/UNC-40 interactions generate an invasive protrusion that crosses the basement membrane. To understand how UNC-40 signals during invasion, we have used genetic, site of action and live-cell imaging studies to examine the roles of known effectors of UNC-40 signaling in axon outgrowth during AC invasion. UNC-34 (Ena/VASP), the Rac GTPases MIG-2 and CED-10 and the actin binding protein UNC-115 (abLIM) are dedicated UNC-40 effectors that are recruited to the invasive membrane by UNC-40 and generate F-actin. MIG-10 (lamellipodin), an effector of UNC-40 in neurons, however, has independent functions from UNC-6/UNC-40. Furthermore, unlike other UNC-40 effectors, its expression is regulated by FOS-1A, a transcription factor that promotes basement membrane breaching. Similar to UNC-40, however, MIG-10 localization to the invasive cell membrane is also dependent on the integrin INA-1/PAT-3. These studies indicate that MIG-10 has distinct functions from UNC-40 signaling in cell invasion, and demonstrate that integrin coordinates invasion by localizing these molecules to the cell-basement membrane interface.

KEY WORDS: MIG-10, Netrin, Integrin, Cell invasion

INTRODUCTION

During development cells must navigate through complex cellular and extracellular matrix environments to disperse, form connections and generate tissues. One of the key barriers that cells encounter is basement membrane, a thin, dense, highly conserved sheet-like matrix that underlies all epithelia and surrounds most tissues (Hynes, 2012; Kalluri, 2003). To overcome this barrier, invasive cells generate and polarize a specialized cell membrane to breach basement membrane (Guo and Giancotti, 2004; Machesky et al., 2008; Ziel et al., 2009). Metastatic cancer cells are thought to utilize the same mechanisms to enable their spread (Rowe and Weiss, 2008). An understanding of how cells traverse basement membranes is limited, however, because of the challenge of recapitulating this behavior faithfully *in vitro* and the difficulty of studying cell-basement membrane interactions in native tissue environments (Even-Ram and Yamada, 2005; Hagedorn and Sherwood, 2011; Hotary et al., 2006; Nourshargh et al., 2010; Wang et al., 2006).

The *C. elegans* gonadal anchor cell (AC) is a uniquely differentiated cell that invades the juxtaposed gonadal and ventral epidermal basement membranes to initiate uterine-vulval connection during larval development (Ihara et al., 2011; Sharma-Kishore et al., 1999; Sherwood and Sternberg, 2003). The highly stereotyped manner of AC invasion and amenability to genetic and visual analysis have recently been utilized to facilitate experimental examination of cell-basement membrane interactions underlying invasion (Hagedorn and Sherwood, 2011). Polarization of the AC towards the basement membrane is regulated by the integrin receptor INA-1/PAT-3, a heterodimer composed of the α-subunit INA-1 paired with the β-subunit PAT-3, which is thought to bind to the basement membrane protein laminin (Baum and Garriga, 1997; Hagedorn et al., 2009). Integrin activity regulates the targeting of the netrin receptor UNC-40 (DCC) to the invasive cell membrane. UNC-40 protein orientation is refined by UNC-6, which is secreted from the ventral nerve cord and accumulates in the basement membrane under the AC (Ziel et al., 2009). UNC-6 (netrin) activation of UNC-40 is further required to generate an invasive protrusion that crosses the basement membrane and intercalates into the neighboring vulval tissue (Hagedorn et al., 2013). Netrin and integrin are strongly associated with invasive cellular activity in development and diseases such as metastatic cancer (Desgrosellier and Cheresh, 2010; Dumartin et al., 2010; Guo and Giancotti, 2004; Kaufmann et al., 2009; Lambert et al., 2012; Nguyen and Cai, 2006), suggesting that these pathways are conserved regulators of cell invasion through basement membrane.

Although both the *unc-6* and *unc-40* genes are essential for the formation of a large invasive protrusion, netrin signaling is not required to breach basement membrane. Loss of *unc-6* and *unc-40* slightly delays, but does not inhibit the ability of the AC to create gaps in the basement membrane (Hagedorn et al., 2013; Ziel et al., 2009). Breaching the basement membrane is dependent on the *C. elegans* ortholog of the vertebrate Fos family transcription factor, FOS-1A, which regulates the expression of genes that mediate basement membrane removal (Sherwood et al., 2005). In *fos-1a* mutants, the AC generates a protrusion that flattens at an intact basement membrane (Sherwood et al., 2005). The effectors acting downstream of FOS-1A and UNC-6/UNC-40 signaling as well as the mechanisms that coordinate their activity at the invasive cell membrane are poorly defined.

An understanding of netrin signaling has primarily been derived from studies in neuronal cells (Gitai et al., 2003; Lebrand et al., 2004; Li et al., 2002a; Quinn et al., 2008; Shekarabi et al., 2005). Thus, to

Department of Biology, Duke University, Science Drive, Box 90388, Durham, NC 27708, USA.

*Author for correspondence (david.sherwood@duke.edu)

Received 9 August 2013; Accepted 9 January 2014

Development (2014) doi:10.1242/dev.102434

further elucidate how netrin signaling promotes AC invasion, we initiated genetic interaction and quantitative imaging studies in the AC on known neuronal effectors of UNC-6/UNC-40. We found that most known neuronal effectors are localized to the invasive cell membrane by UNC-40 and act downstream of UNC-40 signaling during AC invasion. Notably, MIG-10 (lamellipodin), an UNC-6/UNC-40 effector during axon outgrowth and synapse formation (Adler et al., 2006; Chang et al., 2006; Quinn et al., 2006; Stavoe and Colón-Ramos, 2012), was localized and functioned independently of UNC-40. In addition, *mig-10* is transcriptionally regulated by FOS-1A, implicating MIG-10 activity in basement membrane removal. Like UNC-40 (DCC), MIG-10 was also dependent on integrin for localization to the invasive membrane. Together, these results suggest that MIG-10 (lamellipodin) and UNC-6/UNC-40 (netrin signaling) have distinct functions in basement membrane breaching and invasive protrusion formation, respectively, and that integrin targets their localization to the invasive cell membrane.

RESULTS

Effectors of UNC-40 (DCC) in axon guidance promote AC invasion

We have previously shown that UNC-6 (netrin) secreted from ventral nerve cord (VNC) orients UNC-40 (DCC) to the AC-basement membrane interface prior to invasion (Ziel et al., 2009). Furthermore, UNC-6 activation of UNC-40 generates a protrusion that crosses the basement membrane (Hagedorn et al., 2013) (Fig. 1A). We have also observed that UNC-34, the *C. elegans* ortholog of vertebrate Ena/VASP, and two Rac GTPases, MIG-2 and CED-10, are polarized by UNC-6 to this same region. Loss of *unc-34* and the combined loss of *mig-2* and *ced-10* lead to defects in invasion (Ziel et al., 2009). Ena/VASP proteins and Rac GTPases are known downstream effectors of UNC-6/UNC-40 signaling in axon pathfinding and outgrowth (Chang et al., 2006; Gitai et al., 2003; Lebrand et al., 2004; Li et al., 2002b; Shekarabi and Kennedy, 2002), suggesting that netrin signaling might use similar effectors during AC invasion.

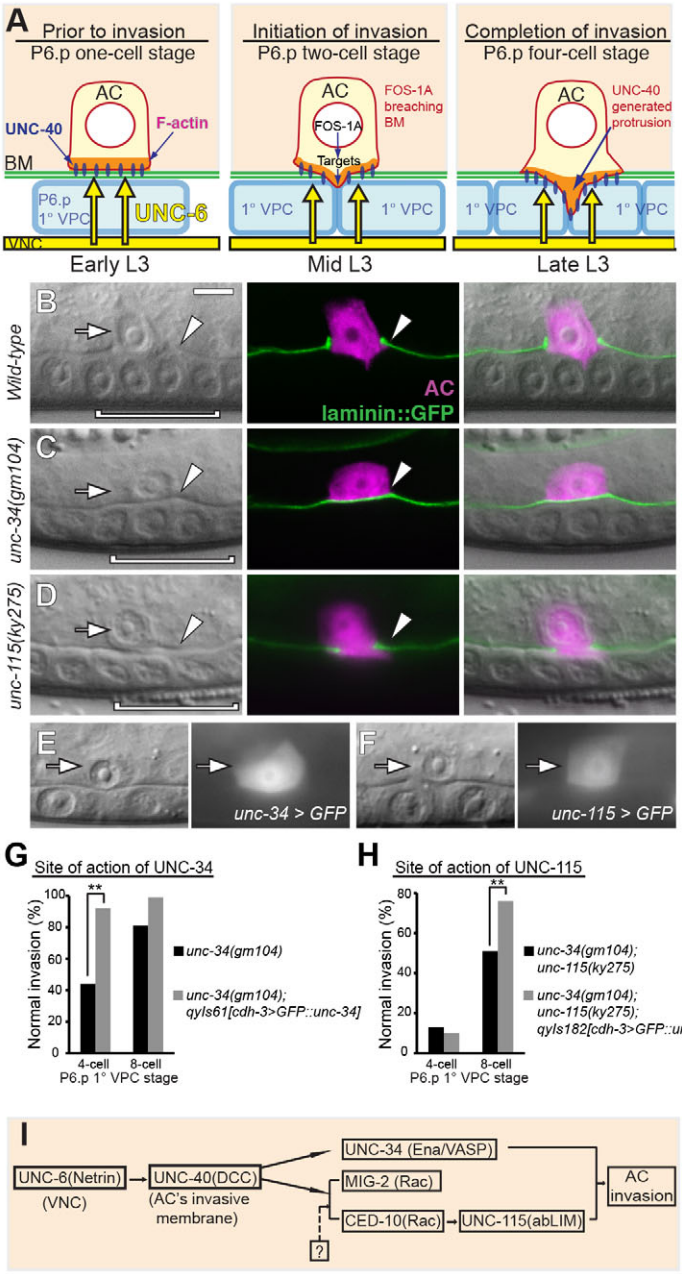

Fig. 1. AC invasion and downstream effectors of UNC-40. Anterior is left; ventral is down; and arrows point to the AC in this and all other figures. (A) A schematic diagram of AC invasion in *C. elegans*. In the early L3 larva the AC is attached to the basement membrane (BM, green) over the primary vulval precursor cell (1° VPC; light blue, P6.p one-cell stage, left). UNC-6 (netrin) (yellow arrows) secreted from the ventral nerve cord (VNC) polarizes its receptor UNC-40 (blue ovals) and F-actin (orange) to the invasive cell membrane in contact with the basement membrane. During the mid-L3, after P6.p divides (P6.p two-cell stage, middle), the AC breaches the basement membrane and generates a protrusion that invades between the two central 1° VPC granddaughter cells by the late L3 (P6.p four-cell stage, right). The transcription factor FOS-1A promotes basement membrane breaching and the UNC-6 receptor UNC-40 mediates protrusion formation. (B-D) DIC images (left), corresponding fluorescence (middle), and overlay (right). (B) In wild-type animals, the AC (arrow, magenta, expressing *zmp-1 >mCherry*) breaches the BM (arrowhead, green, visualized by laminin::GFP) and contacts the central 1° VPCs (bracket) at the P6.p four-cell stage. (C) In this *unc-34* mutant AC invasion failed, leaving the BM intact (arrowhead). (D) In this *unc-115* mutant the AC (arrow) partially removed the BM (arrowhead). (E,F) Transcriptional reporters for *unc-34* (*unc-34* >GFP) and *unc-115* (*unc-115* >GFP) genes are expressed in the AC (arrows) throughout invasion. (G,H) Quantification of the normal percentage invasion of *unc-34* mutants, *unc-34* mutants expressing AC-specific UNC-34, *unc-34;unc-115* double mutants, and *unc-34;unc-115* mutants expressing AC-specific UNC-115 at the P6.p four- and eight-cell stages ($n \geq 50$ for each stage per genotype). We utilized the strong enhancement of *unc-34* by *unc-115* as a sensitive assay for UNC-115 rescue. (I) A diagram of the genetic organization downstream of UNC-6 and UNC-40. As the *ced-10* allele was not null, our genetic analysis cannot rule out that CED-10 and MIG-2 are partially controlled by another signal (question mark). In this and all other figures, $^{*}P<0.05$, $^{**}P<0.01$, $^{***}P<0.001$, N.S., no significant difference (Student's *t*-test). Scale bar: 5 µm.

Development (2014) doi:10.1242/dev.102434

To determine whether UNC-40 engages the same downstream effectors to promote invasion as it does to guide axons, we examined AC invasion in strains with mutations in *unc-34*, *ced-10*, the human *ABLIM1*/limain ortholog *unc-115*, and the lamellipodin ortholog *mig-10* (Lundquist et al., 1998; Manser et al., 1997; Reddien and Horvitz, 2000; Withee et al., 2004; Yu et al., 2002; Zipkin et al., 1997). These genes are established downstream mediators of UNC-40 signaling during axon outgrowth and pathfinding (Chang et al., 2006; Gitai et al., 2003; Quinn et al., 2008). Another Rac GTPase, MIG-2, which often acts redundantly with CED-10 in neuronal development (Demarco et al., 2012; Shakir et al., 2008), was also included for analysis. All alleles examined were putative null mutations except for *ced-10(n1993)*, which is a partial loss-of-function mutation (Reddien and Horvitz, 2000). We scored AC invasion in all assays at the P6.p four-cell stage when basement membrane invasion is completed in wild-type animals (Fig. 1B), and later at the P6.p eight-cell stage (Sherwood and Sternberg, 2003). Of these candidate effectors, we confirmed that *unc-34*, and the two Rac GTPase genes *ced-10* and *mig-2* that act redundantly, promote AC invasion (Fig. 1C; Table 1) (Ziel et al., 2009). We found that loss of a third Rac GTPase, *rac-2*, did not perturb invasion or enhance *mig-2* or *ced-10* defects (data not shown). Animals lacking *unc-115(ky275)* showed a partial block in AC invasion in 8% of ACs examined (Fig. 1D; Table 1), whereas loss of *mig-10(ok2499)* caused a partial invasion in 6% of ACs observed (Table 1). These results indicate that the effectors of UNC-6/UNC-40 in axon development also promote AC invasion.

Ena/VASP (*unc-34*), Rac GTPases (*ced-10* and *mig-2*) and UNC-115 act within the UNC-6/UNC-40 pathway during invasion

To test whether these candidate effectors act within the netrin pathway to regulate invasion, we made double mutant combinations of *unc-40* with each of these genes (Table 1). If these potential effectors function linearly with UNC-40, the double mutants would be predicted to display phenotypic defects similar to those in the *unc-40* single mutants (Wang and Sherwood, 2011). An enhancement of the *unc-40* invasion defect, however, would indicate a function outside of UNC-40 signaling. Loss of *unc-34*, *ced-10*, *mig-2* and *unc-115* did not significantly enhance AC invasion defects caused by *unc-40*, suggesting that these genes function within the UNC-6/UNC-40 (netrin) pathway during AC invasion (Table 1). By contrast, loss of *mig-10* (lamellipodin) strongly enhanced both *unc-40* and *unc-6* defects (Table 1), indicating that *mig-10* has functions outside of UNC-40 signaling.

Effectors of UNC-6/UNC-40 are expressed and function within the AC

We have previously shown that *mig-2* and *ced-10* are expressed and function in the AC to promote invasion (Ziel et al., 2009). To determine where *unc-34* and *unc-115* function, we examined their expression and site of action. Examination of transgenic animals expressing the 5′ *cis*-regulatory elements of *unc-34* and *unc-115* fused to GFP revealed expression in the AC throughout the invasion process (Fig. 1E,F). Supporting the notion that UNC-34 and UNC-115 function in the AC, AC-specific expression of full-length GFP-tagged UNC-34 and UNC-115 (*cdh-3 >GFP::unc-34* and *cdh-3 >GFP::unc-115*) rescued invasion defects caused by their corresponding mutations (Table 1; Fig. 1G,H). We conclude that effectors of UNC-6/UNC-40 signaling function within the AC during invasion.

Effectors of UNC-6/UNC-40 act downstream of the UNC-40 receptor in the AC

Overexpression of UNC-40 in muscles induces randomly directed myopodial extensions in *C. elegans*, suggesting that increased levels of UNC-40 are active, but override polarity cues from UNC-6. Loss of effectors of UNC-40 in muscle arm extension suppresses this phenotype, confirming their function downstream of UNC-40 (Alexander et al., 2009). We similarly found that UNC-40 overexpressed in the AC induced randomly directed protrusions. To determine whether the effectors we identified act downstream of the UNC-40 receptor, we thus determined if their loss suppressed ectopic protrusion formation. As *unc-115* appears to act downstream of *ced-10* in neurons (and in the AC, see below), we examined *ced-10* as a proxy for *unc-115*. Individual loss of *unc-34, mig-2* and *ced-10* dramatically suppressed the length of the ectopic protrusion (Fig. 2A-G), indicating that these effectors can act downstream of UNC-40 in the AC. Further supporting a downstream function, we found that UNC-40::GFP was polarized normally in *unc-34* mutants and in *mig-2(mu28)* animals treated with *ced-10 RNAi* (Fig. 2H-K).

Effectors of UNC-6/UNC-40 function within two branches to regulate AC invasion

Genetic and molecular studies in *C. elegans* have indicated that two distinct pathways act downstream of UNC-40 signaling during axon outgrowth and turning (Gitai et al., 2003). One pathway is mediated by UNC-34, and the other is composed of CED-10 and UNC-115. Consistent with a similar organization in the AC, the *unc-34* mutant invasion defects were enhanced by loss of *unc-115* as well as reduction of *ced-10* by RNAi (Table 1). Furthermore, loss of *mig-2* also enhanced *unc-34* mutants (Table 1). These results suggest UNC-34 also functions in a distinct branch downstream of UNC-40 signaling in the AC (summarized in Fig. 1I).

We then examined genetic interactions between *mig-2*, *ced-10* and *unc-115*. Loss of *mig-2* significantly enhanced the *unc-115* mutant phenotype, indicating parallel activities. By contrast, *ced-10(n1993)* did not enhance loss of *unc-115*, suggesting that *ced-10* and *unc-115* function in a linear pathway. These results are consistent with studies on axon pathfinding and outgrowth, suggesting that the actin binding protein UNC-115 acts downstream of CED-10 and in parallel to MIG-2 (Fig. 1I) (Demarco and Lundquist, 2010; Gitai et al., 2003; Struckhoff and Lundquist, 2003).

Effectors of UNC-40 promote F-actin formation at the invasive cell membrane of the AC

Ena/VASP proteins, Rac GTPases and abLIM/limatin are known regulators of actin cytoskeletal signaling (Bear and Gertler, 2009; Burridge and Wennerberg, 2004; Struckhoff and Lundquist, 2003). This suggests that UNC-34 (Ena/VASP), the Rac GTPases MIG-2 and CED-10, and UNC-115 (abLIM) may help organize the F-actin network downstream of UNC-40 signaling during invasion. We thus examined the localization and volume of the integrated fluorescence intensity of the F-actin probe mCherry::moeABD in animals harboring mutations in these genes. Compared with wild-type ACs where F-actin was tightly polarized to the invasive cell membrane, we found that 22% of the total amount of F-actin was mislocalized to the apical and lateral membranes of ACs in *unc-34* mutants (Fig. 3A,B,E). In addition, the overall volume of F-actin in *unc-34* mutants was reduced by ~50% (Fig. 3F). Reduction of the activity in the Rac GTPase branch of UNC-40 signaling [*mig-2(mu28);ced-10(RNAi)*] did not alter the polarity of F-actin, but led to a 65% reduction of F-actin volume (Fig. 3A,C,E,F). Notably, loss of *mig-10*, which has functions outside UNC-40 signaling in the AC, did

Development (2014) doi:10.1242/dev.102434

Table 1. Genetic analysis of the netrin pathway, *mig-10*, integrin and the FOS-1 pathway during AC invasion

	AC invasion*							
	P6.p 4-cell stage (mid-to-late L3 stage)				P6.p 8-cell stage (early L4 stage)			
Genotype/treatment	Full invasion (%)	Partial invasion (%)	No invasion (%)	*n*	Full invasion (%)	Partial invasion (%)	No invasion (%)	*n*
UNC-6/UNC-40 pathway effectors								
Wild type (N2)	100	0	0	>100	100	0	0	>100
unc-40(e271)	5	29	66	56	52	38	10	61
unc-6(ev400)	14	14	72	51	44	38	18	72
unc-34(gm104)	44	38	18	50	81	19	0	63
unc-34(e951)	33	64	3	58	85	15	0	54
mig-2(mu28)	100	0	0	54	100	0	0	64
ced-10(n1993)	98	2	0	61	100	0	0	57
mig-2(mu28);ced-10(RNAi)	62	21	17	24	85	15	0	41
unc-115(ky275)	92	8	0	51	100	0	0	63
mig-10(ok2499)	94	6	0	51	100	0	0	52
mig-10(ct41)	98	2	0	51	100	0	0	52
Effectors and UNC-40								
unc-40(e271);unc-34(gm104)‡	0	26	74	47	45	31	24	51
unc-40(e271);mig-2(mu28)‡	6	31	63	51	47	50	3	64
unc-40(e271);ced-10(n1993)‡	4	16	80	50	44	29	27	55
unc-40(e271);mig-2(mu28);ced-10(RNAi)‡	2	16	82	50	31	49	20	49
unc-40(e271);unc-115(ky275)‡	0	25	75	51	46	38	16	78
unc-40(e271);mig-10(ct41)§	0	6	94	49	8	44	48	72
unc-6(ev400);mig-10(ct41)¶	0	6	94	47	4	25	71	84
Interactions among effectors								
*unc-34(e951);mig-2(mu28)***	0	32	68	34	26	65	9	57
unc-34(gm104);ced-10(RNAi)‡‡	39	20	41	51	70	25	5	67
*unc-34(gm104);unc-115(ky275)***	13	27	60	52	51	49	0	76
mig-2(mu28);unc-115(ky275)§§	61	33	6	51	82	18	0	56
ced-10(n1993);unc-115(ky275)¶¶	86	14	0	51	100	0	0	54
Site of action								
*unc-34(gm104);qyIs61[cdh-3>GFP::unc-34]****	92	8	0	50	99	1	0	75
unc-34(gm104);unc-115(ky275);qyIs182[cdh-3>GFP::unc-115]‡‡‡	10	12	78	50	76	24	0	63
unc-6(ev400);mig-10(ct41);qyIs183[cdh-3>mig-10b::GFP]§§§	4	14	82	50	15	52	33	58
mig-10 interaction with integrin								
rrf-3(pk1426)	100	0	0	50	100	0	0	75
rrf-3(pk1426);ina-1(RNAi)	86	4	10	92	99	0	1	71
rrf-3(pk1426);ina-1(RNAi);mig-10(ct41)¶¶¶	69	13	18	89	93	6	1	71
mig-10 interaction with FOS-1 target								
him-4(rh319)	86	4	10	51	100	0	0	52
*mig-10(ct41);him-4(rh319)*****	66	16	18	50	75	25	0	53

*Normal invasion, partial invasion and no invasion were defined by the degree to which the BM underneath of the AC was interrupted (see Fig. 1). BM integrity was examined using DIC optics as previously shown (Sherwood and Sternberg, 2003).
Statistical comparison of scoring results (Fisher's exact test; full invasion versus defective invasion, unless noted otherwise):
‡compared with *unc-40(e271)*, $P>0.1$ at the P6.p four-cell stage;
§compared with *unc-40(e271)*, $P<0.01$ at the four-cell stage (partial invasion versus no invasion);
¶compared with *unc-6(ev400)*, $P<0.01$ at the four-cell stage (partial invasion versus no invasion);
**compared with *unc-34(gm104)*, $P<0.01$ at the four-cell stage; compared with *unc-40(e271)*, $P>0.1$ at the P6.p four-cell stage;
‡‡compared with *unc-34(gm104)*, $P<0.01$ at the four-cell stage (partial invasion versus no invasion); compared with *unc-40(e271)*, $P<0.01$ at the four- and eight-cell stages;
§§compared with *unc-115(ky275)*, $P<0.01$ at the four-cell stage;
¶¶compared with *unc-115(ky275)*, $P>0.1$ at the four-cell stage;
***compared with *unc-34(gm104)*, $P<0.01$ at the four- and eight-cell stages, indicating a rescue;
‡‡‡compared with corresponding double mutants, $P>0.1$ at the four-cell stage (full invasion versus defective invasion) and $P>0.07$ (partial invasion versus no invasion); $P<0.01$ at the eight-cell stage, indicating a partial rescue;
§§§compared with corresponding double mutants, $P>0.05$ at the eight-cell stage, indicating a partial rescue;
¶¶¶compared with *rrf-3(pk1426);ina-1(RNAi)*, $P<0.01$ at the four-cell stage;
****compared with *him-4(rh319)*, $P<0.05$ at the four-cell stage.

not affect F-actin polarity or volume (Fig. 3D-F). Taken together, these results indicate that dedicated effectors of UNC-40 signaling function to promote F-actin formation, with UNC-34 also having a role in regulating F-actin polarity.

UNC-40 polarizes its effectors to the invasive cell membrane

UNC-6 (netrin) orients UNC-40, F-actin and the actin regulators UNC-34, CED-10 and MIG-2 to the invasive cell membrane of the

Development (2014) doi:10.1242/dev.102434

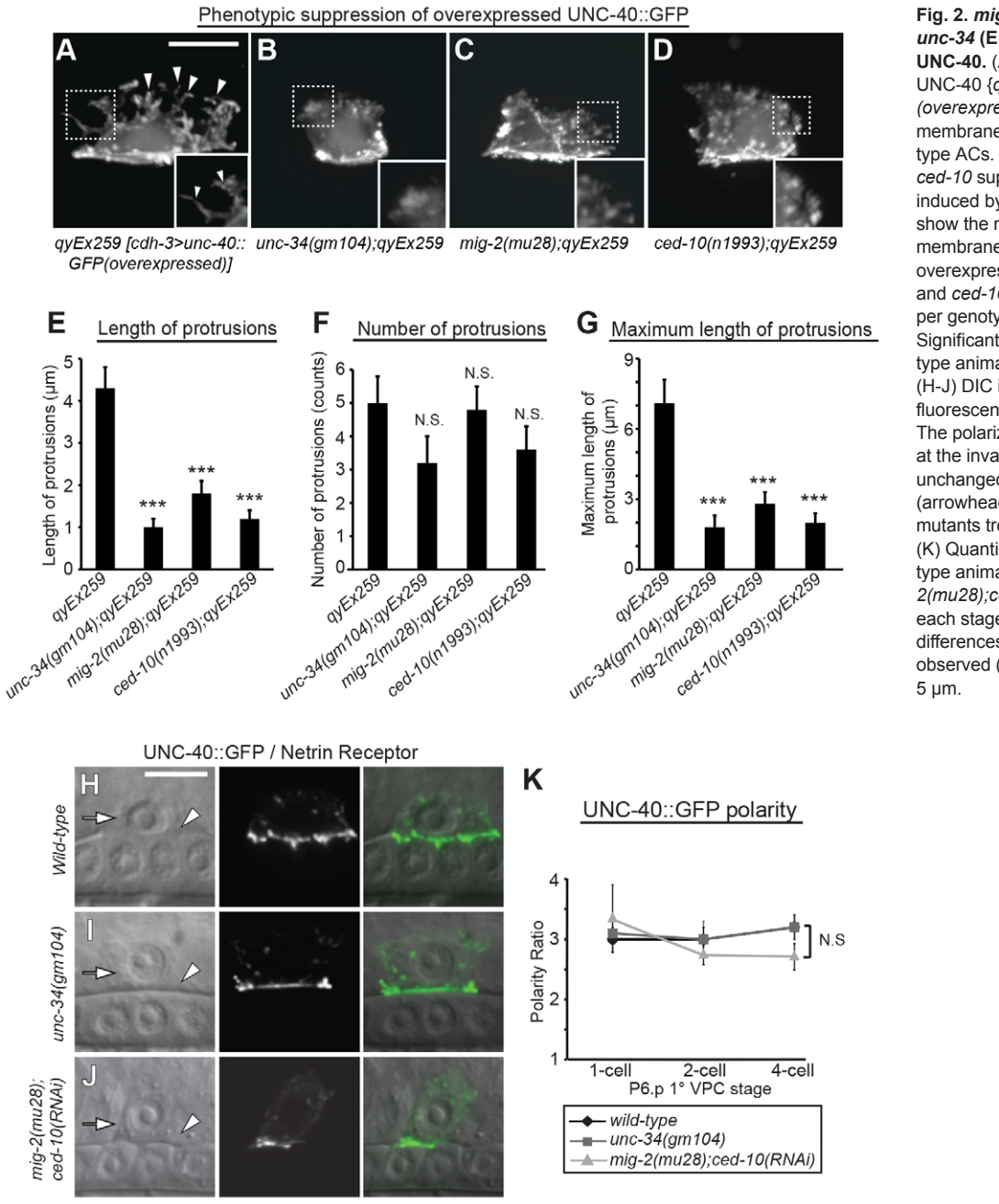

Fig. 2. *mig-2*, *ced-10* (Rac GTPases) and *unc-34* (Ena/VASP) act downstream of UNC-40. (A) AC-specific overexpression of UNC-40 {*qyEx259 [cdh-3 >unc-40::GFP (overexpressed)]*} induced ectopic membrane protrusions (arrowheads) in wild-type ACs. (B-D) Loss of *unc-34, mig-2* and *ced-10* suppressed the protrusive phenotype induced by UNC-40 overexpression. Insets show the morphological changes in the AC membrane. (E-G) Quantification of UNC-40 overexpression phenotype in *unc-34*, *mig-2* and *ced-10* mutants ($n \geq 15$ for each stage per genotype). Error bars indicate s.e.m. Significant differences compared with wild-type animals are indicated (Student's *t*-test). (H-J) DIC images (left), corresponding fluorescence (middle), and overlay (right). The polarized localization of UNC-40::GFP at the invasive cell membrane remained unchanged in ACs that failed to invade (arrowheads) in *unc-34* mutants and *mig-2* mutants treated with *ced-10* RNAi. (K) Quantification of UNC-40 polarity in wild-type animals, *unc-34* mutants and *mig-2(mu28);ced-10(RNAi)* animals ($n \geq 15$ for each stage per genotype). No significant differences relative to wild type were observed (Student's *t*-test). Scale bars: 5 µm.

AC prior to invasion (Ziel et al., 2009). To provide a more complete understanding of the localization of UNC-40 effectors, we first determined the subcellular localization of UNC-115 in the AC. Similar to UNC-34, CED-10 and MIG-2, AC-specific expression of GFP-tagged UNC-115 showed that UNC-115 was first localized to the basal invasive membrane, approximately 5 hours prior to invasion and its polarity increased throughout AC invasion (Fig. 4A,I). We next determined whether UNC-40 functions to localize its effectors at the invasive cell membrane. Consistent with their genetic placement downstream of *unc-40*, UNC-115 and UNC-34 showed an approximate 50% reduction in polarity in *unc-40* mutants (Fig. 4A,B,E,F,I), and the Rac GTPases CED-10 and MIG-2 had an approximate 70% reduction in polarity (Fig. 4C,D,G-I). We conclude that UNC-40 promotes the localization of its dedicated effectors to the invasive cell membrane of the AC.

mig-10b, but not dedicated UNC-40 effectors, are transcriptionally regulated by FOS-1A

Loss of *mig-10* strongly enhanced the invasion defects in *unc-40* and *unc-6* mutants (Table 1), suggesting that MIG-10 has functions outside UNC-6/UNC-40 signaling that contribute to invasion. We were next interested in understanding how MIG-10 regulates AC invasion. The *mig-10* gene encodes three protein isoforms, MIG-10A-C (Manser et al., 1997; Quinn et al., 2006; Stavoe et al., 2012). Using reporters consisting of upstream 5′ *cis*-regulatory elements (CRE) to drive GFP (3.5 kb, 2.9 kb and 4 kb immediately upstream of ATG start codons of *mig-10a*, *mig-10b* and *mig-10c*, respectively), we found that the 5′ CRE of *mig-10a* drove expression in uterine cells surrounding the AC, but was not detectable in the AC (Fig. 5A). *mig-10c* was expressed in ventral uterine cells and neurons of the ventral nerve cord, and was also absent from the AC (Fig. 5B). Notably, the 5′ CRE for *mig-10b* was specifically

Development (2014) doi:10.1242/dev.102434

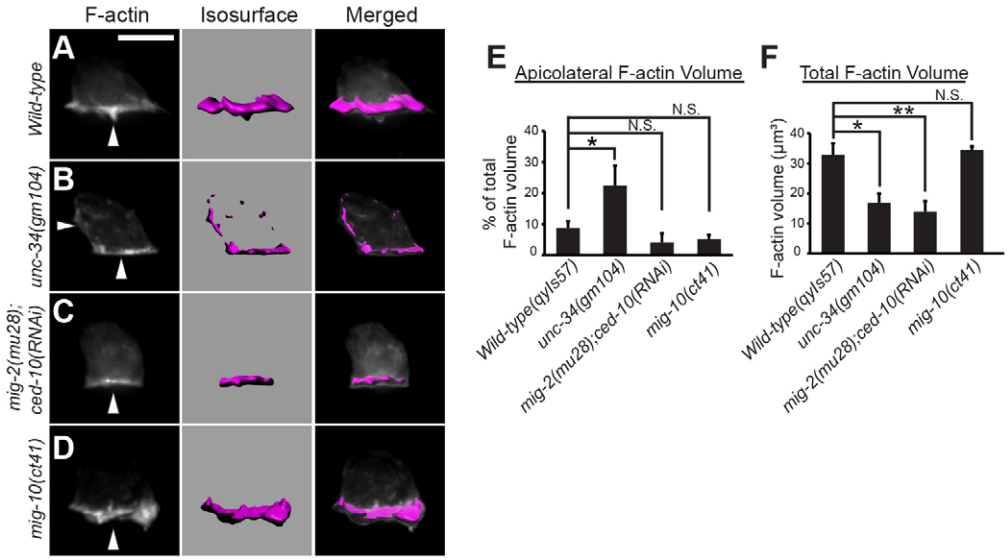

Fig. 3. UNC-34 (Ena/VASP), and the Rac GTPases MIG-2 and CED-10 promote F-actin formation at the invasive cell membrane of the AC. (A-D) Images show three-dimensional reconstructions generated from confocal *z*-stacks taken in animals at the P6.p four-cell stage. Fluorescence (left), corresponding dense F-actin network rendered with isosurfaces (middle), overlay (right). (A) In wild-type animals, the F-actin-binding probe (mCherry::moeABD) localized to the invasive cell membrane (arrowhead). (B) In *unc-34* mutants, F-actin was reduced and mislocalized to the apical and lateral membranes of the AC (arrowheads). (C) In *mig-2(mu28);ced-10(RNAi)* animals, F-actin was reduced but remained polarized (arrowhead). (D) In *mig-10* mutants the levels and localization of F-actin were normal (arrowhead). (E) The percentage of the total volume of F-actin that localized apicolaterally at the P6.p four-cell stage ($n \geq 15$ per genotype). (F) The total volume of the F-actin at the P6.p four-cell stage ($n \geq 12$ per genotype). The overall volume of F-actin in *unc-34* mutants was reduced by ~50% compared with wild-type animals, whereas reduction of the activity in the Rac GTPases led to a 65% reduction of F-actin. Significant differences relative to wild-type animals are indicated (Student's *t*-test). Scale bar: 5 µm.

expressed in the AC throughout invasion (Fig. 5C), suggesting that the *mig-10b* isoform regulates AC invasion. Consistent with this idea, AC-specific expression of MIG-10B had rescuing activity in the *unc-6;mig-10* double mutant (we utilized *mig-10* enhancement of the *unc-6* mutant phenotype as a more sensitive basis to determine rescue; Table 1; Fig. 5I). Thus, MIG-10B functions in the AC to promote invasion.

Outside of UNC-6/UNC-40 signaling, the transcriptional regulator *fos-1a* plays a distinct role in AC invasion. FOS-1A regulates the expression of genes that promote breaching of the basement membrane, but it does not regulate protrusion formation (Sherwood et al., 2005). To test if *mig-10b* functions in the FOS-1A pathway, we examined the expression of *mig-10b* in animals treated with *fos-1* RNAi. Strikingly, loss of *fos-1* led to a complete absence of detectable *mig-10b* expression in the AC (n=19/19 animals; Fig. 5D). FOS-1A is thought to regulate diverse targets that function together to promote basement membrane removal (Sherwood et al., 2005). Loss of these genes leads to additive invasion defects. Consistent with MIG-10B acting as a functional target of FOS-1A, loss of *mig-10* enhanced the invasion defect of the matrix component hemicentin (*him-4*), a FOS-1A transcriptional target that promotes basement membrane removal (Table 1) (Sherwood et al., 2005).

We next determined whether the expression of the dedicated netrin pathway effectors are controlled by FOS-1A. The expression of the Rac GTPase *mig-2* in the AC is not regulated by FOS-1A (Sherwood et al., 2005). Similarly, we found that *ced-10*, *unc-115* and *unc-34* were still expressed in the AC after loss of *fos-1* ($n \geq 10$ animals examined for each; supplementary material Fig. S1). These results are consistent with our genetic studies, indicating that these effectors function specifically within the netrin pathway to promote invasion. Taken together, these data suggest that *mig-10b* is a component of the FOS-1A transcriptional pathway, which promotes basement membrane breaching.

MIG-10B localization to the invasive membrane is independent of UNC-40, but requires integrin

We next examined a functional translational fusion of GFP to MIG-10B to determine where it is localized in the AC. Consistent with a role in promoting basement membrane breaching, MIG-10B was strongly polarized to the invasive cell membrane prior to invasion (Fig. 5E,J). Unlike dedicated UNC-6 and UNC-40 effectors, however, MIG-10B polarization was not dependent on UNC-40 (Fig. 5F,J; supplementary material Fig. S2). In both the HSN and AIY neurons, MIG-10 localization is regulated through netrin signaling by the Rac GTPase CED-10 (Quinn et al., 2008; Stavoe and Colón-Ramos, 2012). Consistent with netrin-independent localization, MIG-10B was polarized normally at the invasive cell membrane of the AC in *ced-10* (n1993) mutant animals (supplementary material Fig. S3). These results indicate that another polarity pathway plays a primary role in directing the polarized localization of MIG-10B in the AC.

The only other known polarity system regulating invasive membrane polarization during AC invasion is the integrin heterodimer INA-1/PAT-3 (Hagedorn et al., 2009). INA-1/PAT-3 functions upstream of UNC-40 (DCC) and is required for UNC-40 targeting to the invasive cell membrane (Hagedorn et al., 2009). We thus examined whether MIG-10B localization is dependent on INA-1/PAT-3 activity. Null mutations in *ina-1* cause L1 larval lethality (Baum and Garriga, 1997). We therefore examined animals containing a hypomorphic, viable mutation in *ina-1*: *ina-1(gm39)* (Baum and Garriga, 1997). *ina-1(gm39)* mutants had a 50% reduction in MIG-10B polarity (Fig. 5G,J), demonstrating that INA-1 mediates MIG-10B localization to the invasive membrane. To determine if INA-1/PAT-3 functioned cell autonomously to promote MIG-10B localization, we examined MIG-10B in animals expressing a previously characterized dominant-negative integrin specifically driven in the AC (*zmp-1 >HA-βtail*) (Hagedorn et al.,

Development (2014) doi:10.1242/dev.102434

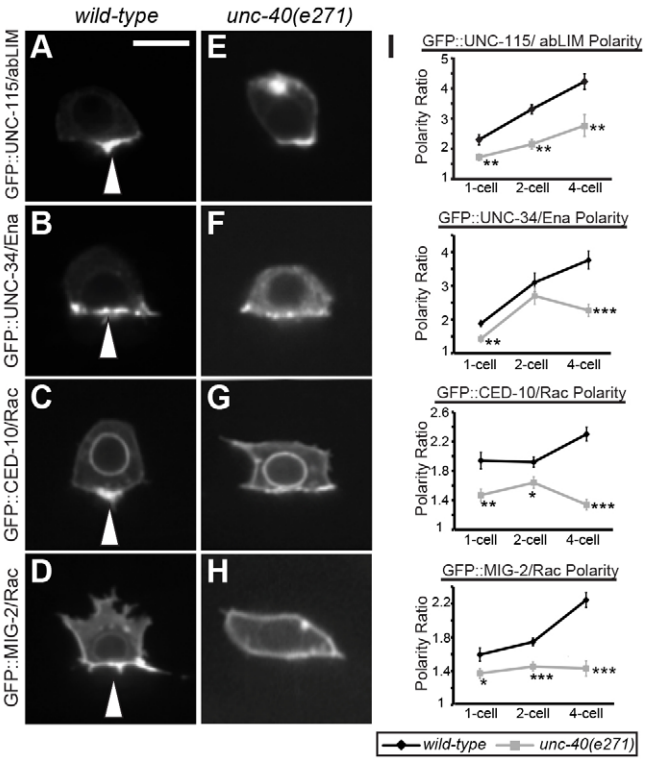

Fig. 4. UNC-40 polarizes its effectors to the invasive cell membrane. All animals were examined at the P6.p four-cell stage. (A-D) In wild-type animals, GFP fusion proteins for UNC-115, UNC-34, CED-10 and MIG-2 localized to the invasive membrane (arrowheads). (E-H) In *unc-40* mutants, the polarized localization of UNC-115, UNC-34, CED-10 and MIG-2 was disrupted. (I) Quantification of UNC-115, UNC-34, CED-10 and MIG-2 polarization to the invasive cell membrane in wild-type animals (black diamonds) and *unc-40* mutants (gray squares; $n \geq 15$ for each stage per genotype). Significant differences relative to wild-type animals are indicated (Student's *t*-test). Scale bar: 5 µm.

2009; Lee et al., 2001). Consistent with a cell-autonomous role, MIG-10B targeting to the invasive membrane was dramatically reduced in *zmp-1 >HA-βtail* animals (Fig. 5H,J). Importantly, reduction of either *ina-1* or *pat-3* activity resulted in loss of MIG-10B targeting, while still maintaining AC-basement membrane adhesion (Fig. 5H) (Hagedorn et al., 2009). Thus, INA-1/PAT-3 has a role in targeting MIG-10B to the invasive cell membrane, independent of AC-basement membrane adhesion.

The MIG-10 isoforms A, B and C differ only in their N-terminal domain and this region has been postulated to dictate interactions that drive specific subcellular localization (Stavoe et al., 2012). Supporting this idea, we found that expression of a GFP-tagged form of MIG-10B lacking its unique N-terminal domain [MIG-10B(ΔN)::GFP] reduced the ability of MIG-10 to localize to the invasive cell membrane (supplementary material Fig. S4). Loss of *unc-40* did not further decrease polarization of this construct (supplementary material Fig. S4). We conclude that MIG-10B localizes to the invasive cell membrane in an integrin-dependent manner that is regulated in part by its unique N-terminal domain.

INA-1/PAT-3 (integrin) localization to the invasive membrane is not regulated by FOS-1A

Our analysis suggested that INA-1/PAT-3 regulates the localization of at least two distinct signaling activities at the invasive cell membrane: UNC-40 (invasive protrusion formation) and MIG-10B, which has a UNC-40/UNC-6 independent function as a FOS-1A target promoting basement membrane removal. Further supporting the idea that integrin localizes signaling molecules at the invasive membrane, INA-1/PAT-3 is also required for the localization of the UNC-40 effector MIG-2 (Hagedorn et al., 2009) and the UNC-40 effectors UNC-34 and UNC-115 (supplementary material Fig. S5). These studies support a model in which INA-1/PAT-3 targets the localization of multiple signaling molecules to the invasive membrane where they function during invasion.

Loss of UNC-6/UNC-40 (netrin) signaling does not control INA-1/PAT-3 localization at the invasive membrane, consistent with a role for UNC-40 downstream of integrin activity (Hagedorn et al., 2009). We thus next examined whether FOS-1A activity regulates INA-1/PAT-3 localization. Similar to *Drosophila* and vertebrates, the *C. elegans* α-INA-1 and β-PAT-3 subunits require association within the secretory apparatus to be transported to the cell surface (Hagedorn et al., 2009; Leptin et al., 1989; Marlin et al., 1986). Therefore, we examined the expression of an INA-1/PAT-3 reporter from worms expressing genomic DNA encoding *ina-1* and genomic DNA encoding *pat-3* tagged with GFP. INA-1/PAT-3::GFP was transported to the surface of ACs and polarized to the invasive cell membrane (Fig. 6A,C). Loss of *fos-1* did not reduce or alter the polarized localization of INA-1/PAT-3::GFP (Fig. 6B,C). These results indicate that FOS-1A activity does not regulate INA-1/PAT-3 expression or localization at the invasive membrane.

To further test the idea that integrin regulates multiple signaling activities at the invasive cell membrane, we examined genetic interactions between *mig-10b* and integrin. A synergistic interaction would be consistent with INA-1/PAT-3 (integrin) regulating the activity of other signaling pathways (such as netrin) that are crucial to invasion (Pérez-Pérez et al., 2009). Supporting this hypothesis, animals harboring a null mutation of *mig-10*, treated with *ina-1(RNAi)* had a defect in AC invasion greater than the additive loss of *mig-10* and *ina-1(RNAi)* (Table 1). Taken together, these results support the notion that INA-1/PAT-3 mediates the localization and function of distinct signaling pathways at the invasive cell membrane of the AC.

DISCUSSION

The signaling mechanisms that cells utilize to cross basement membranes are poorly understood. Using the model of AC invasion in *C. elegans*, we reveal downstream effectors of two pathways that are conserved regulators of invasion: the netrin pathway, which organizes a cellular protrusion that crosses the basement membrane; and the FOS-1A transcription pathway, which regulates the expression of genes that promote basement membrane breaching. Furthermore, we show that the integrin receptor INA-1/PAT-3 localizes effectors of these pathways to the invasive front, suggesting that integrin coordinates distinct cellular behaviors that contribute to invasion (summarized in Fig. 7).

UNC-6/UNC-40 effectors during AC invasion

Although the UNC-6 (netrin)/UNC-40 (DCC) pathway mediates many diverse morphogenetic processes (Adler et al., 2006; Colón-Ramos et al., 2007; Hedgecock et al., 1990; Lai Wing Sun et al., 2011; Teichmann and Shen, 2011; Ziel et al., 2009), how netrin signals in cells other than neurons remains poorly understood. We have found that the effectors downstream of the netrin receptor UNC-40 during AC invasion are largely shared and show a similar genetic organization to those identified in *C. elegans* neuronal pathfinding and outgrowth. Specifically, the pathway downstream of UNC-40 signaling in AC invasion also has at least two branches:

Development (2014) doi:10.1242/dev.102434

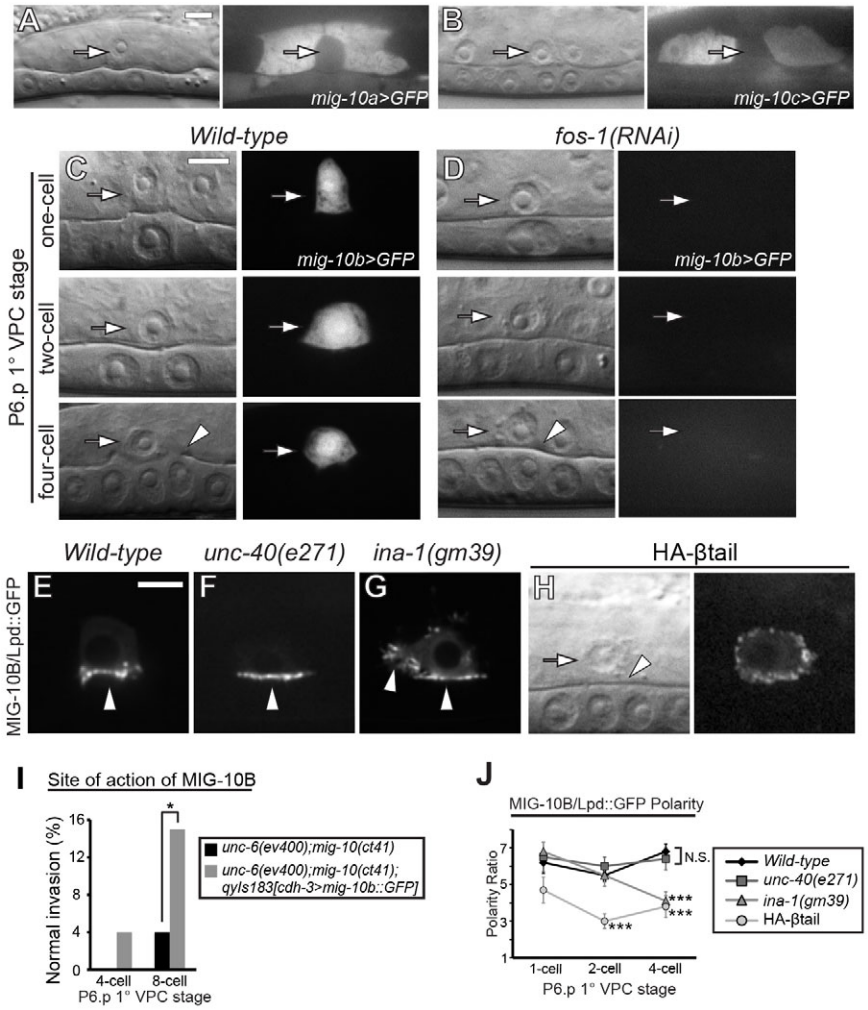

Fig. 5. Integrin localizes MIG-10B, a transcriptional target of FOS-1A. (A-D,H) DIC images (left), corresponding fluorescence (right). (A-C) *mig-10* isoform expression in uterine and vulval tissues during AC invasion. (A) The 5′ CRE of *mig-10a* (*mig-10a >GFP*) drove expression in most uterine cells, but was not detectable in the AC (arrows). (B) *mig-10c* (*mig-10c >GFP*) was expressed in ventral uterine cells, but was absent from the AC (arrows). (C) The 5′ CRE of *mig-10b (mig-10b >GFP)* drove specific expression in the AC prior to and during invasion (arrows). (D) RNAi targeting *fos-1a* eliminated detectable *mig-10b* expression in the AC (arrows). (E) In wild-type ACs, MIG-10B::GFP (*cdh-3 >mig-10b::GFP*) was polarized to the invasive cell membrane (arrowhead). (F) MIG-10B::GFP was polarized normally in *unc-40(e271)* animals (arrowhead). (G) MIG-10B::GFP polarity was significantly reduced in *ina-1(gm39)* mutants (arrowheads). (H) Expression of a dominant-negative integrin PAT-3 β-subunit in the AC (*zmp-1 >HA-βtail*, arrow) reduced MIG-10B polarization. ACs in *HA-βtail* animals still adhered to the underlying basement membrane (arrowhead, DIC image). (I) Quantification of the normal invasion percentage of *unc-6;mig-10* mutants and *unc-6;mig-10* expressing AC-specific MIG-10B ($n \geq 50$ for each stage per genotype). (J) Quantification of MIG-10B polarization to the invasive cell membrane in wild-type animals (black diamonds), *unc-40* mutants (dark gray squares), *ina-1* mutants (dark gray triangles) and *HA-βtail* (gray circles; $n \geq 15$ for each stage per genotype). Significant differences relative to wild-type animals are indicated (Student's *t*-test). Scale bars: 5 µm.

one containing UNC-34 and the other composed of the Rac GTPase CED-10 and the actin-binding protein UNC-115 (Chang et al., 2006; Demarco and Lundquist, 2010; Gitai et al., 2003; Teichmann and Shen, 2011). Our data also suggest that the Rac GTPase MIG-2, which appears to act redundantly with CED-10 (Demarco et al., 2012), is in this branch. We show that these effectors function in the AC, UNC-40 directs their localization to the invasive cell membrane of the AC, and that they promote F-actin formation, which is probably necessary to generate an invasive protrusion that penetrates the basement membrane. The shared downstream effectors of UNC-40 between neurons and the AC suggest that this may be a core set of UNC-40 effectors and that UNC-40 has similarities in how it signals in diverse contexts.

MIG-10B is a target of FOS-1A regulation in the AC

MIG-10 is a member of the MRL (MIG-10, RIAM and lamellipodin) family of multi-adaptor proteins that mediate cell adhesion and migration (Coló et al., 2012; Lafuente et al., 2004). Recent studies examining the three isoforms (A-C) of MIG-10 in *C. elegans* have revealed that their unique N-terminal regions influence their localization and function (Stavoe et al., 2012). In response to UNC-6 (netrin), MIG-10A and MIG-10B are asymmetrically localized and are thought to organize the cytoskeleton to mediate axon outgrown and guidance (Adler et al., 2006; Chang et al., 2006; Quinn et al., 2008). Furthermore, UNC-6 and the active zone proteins SYD-1 and SYD-2 localize MIG-10B to presynaptic sites, which in turn direct synaptic vesicle clustering (Stavoe et al., 2012). Our genetic and cell biological results revealed that the *mig-10b* isoform is specifically expressed in the AC, but that it is not a dedicated effector of UNC-40 signaling. Importantly, our data does not rule out a function for MIG-10B acting as an effector of UNC-40, but it does show that it has functions other than netrin signaling. Our data point to an UNC-40-independent role for MIG-10B as a regulator of basement membrane removal. Unlike dedicated UNC-40 effectors, *mig-10b* expression in the AC was dependent on the transcription factor FOS-1A, which controls the expression of genes that promote basement membrane removal. A further distinction from dedicated UNC-40 effectors was that MIG-10B localization to the invasive membrane was not dependent on UNC-40. Instead MIG-10B was targeted to the invasive cell membrane by the extracellular matrix receptor INA-1/PAT-3 (integrin). Interestingly, the earliest characterization of *mig-10* mutant animals suggested that MIG-10 might have functions in cell-matrix interactions during excretory canal outgrowth and cell migration (Manser and Wood, 1990). Furthermore, MIG-10 is known to have functions other than a dedicated effector of netrin signaling (Quinn et al., 2006). It is not well understood how MRL proteins localize to specific membrane regions (Coló et al., 2012; Stavoe et al., 2012). The unique N-terminus of MIG-10B is predicted to adopt an amphipathic α-helix conformation, which mediates binding of the vertebrate MRL protein RIAM to talin (Coló et al., 2012; Lee et al., 2009). Given that talin links integrin to the actin cytoskeleton, it is possible that

Development (2014) doi:10.1242/dev.102434

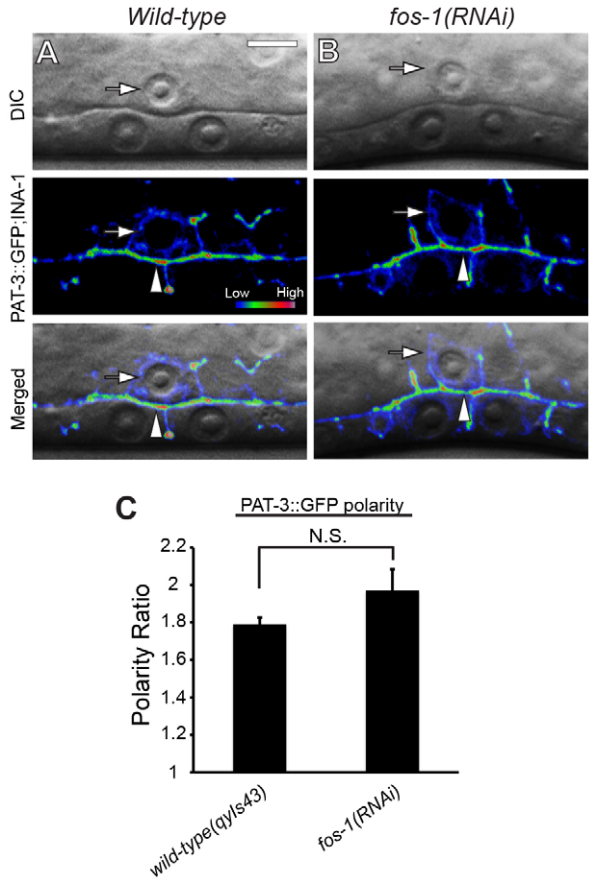

Fig. 6. Integrin localization is independent of *fos-1a* in the AC. DIC images (upper panels), spectral representation of fluorescent intensity (middle), and overlay (lower) are shown of single confocal sections through the AC. (A) In wild-type ACs (arrows), the integrin INA-1/PAT-3 (visualized by PAT-3::GFP;INA-1) localized to the invasive cell membrane (arrowhead) in contact with the basement membrane. (B) PAT-3::GFP localization remained unchanged (arrowhead) in the AC (arrows) after reduction of *fos-1* by RNAi. (C) Quantification of PAT-3::GFP polarization to the invasive cell membrane of the AC at the P6.p four-cell stage in wild type and in animals treated with *fos-1* RNAi ($n \geq 10$ for each). No significant differences relative to wild type were observed (Student's *t*-test). Scale bar: 5 µm.

MIG-10B is targeted to the invasive cell membrane of the AC by a close association with INA-1/PAT-3. Alternatively, integrins are known to regulate the cytoskeleton (Legate et al., 2009), as well as vesicular trafficking (Caswell et al., 2009), both of which might promote the localization of MIG-10B to the invasive membrane.

Fos family transcription factors are conserved regulators of invasion and have been implicated in regulating a battery of genes that contribute to basement membrane breaching (Luo et al., 2010; Matus et al., 2010; Milde-Langosch, 2005; Ozanne et al., 2007; Sherwood et al., 2005; Uhlirova and Bohmann, 2006; Young and Colburn, 2006). Several FOS-1A targets in the AC have been identified, including the extracellular matrix protein hemicentin, which is deposited in the basement membrane prior to invasion. Another FOS-1A target is the matrix metalloproteinase *zmp-1*, which has homology to proteases implicated in basement membrane degradation in vertebrates, but localization of which at the invasive membrane is not well understood (Sherwood et al., 2005). Similar to *mig-10b*, loss of hemicentin leads to only a weak defect in AC invasion. In addition, mutants in *zmp-1* have no apparent invasion defect (Sherwood et al., 2005). Given the fully penetrant flattening of the invasive protrusion at an intact basement membrane in *fos-1a* mutants (Sherwood et al., 2005), these observations suggest that the diverse targets of FOS-1A regulation have redundant or modulatory roles that function together to breach basement membrane.

Integrin localizes distinct signaling activities to the invasive cell membrane

Integrin expression and activity are strongly associated with cell invasion through the basement membrane in vertebrates (Desgrosellier and Cheresh, 2010; Guo and Giancotti, 2004). The presence of at least 24 integrin heterodimers in vertebrates, as well as the complexity of the tissues, has hindered experimental dissection of the functions of these receptors during cell invasion *in vivo* (Bader et al., 1998; Brockbank et al., 2005; Felding-Habermann, 2003; Sixt et al., 2006). The *C. elegans* genome encodes only two predicted integrin receptors (Kramer, 2005) and only one of these, INA-1/PAT-3, is expressed and functions in the AC (Hagedorn et al., 2009). Loss of *ina-1* or *pat-3* strongly blocks AC invasion, but only slightly reduces AC-basement membrane contact (Hagedorn et al., 2009). This observation indicates that INA-1/PAT-3 has roles in promoting invasion beyond AC-basement membrane adhesion. Previously, it has been shown that INA-1/PAT-3 functions upstream of UNC-40 to regulate the targeting of UNC-40 to the invasive cell membrane (Hagedorn et al., 2009). Our results here extend these findings to the *fos-1a* transcriptional target MIG-10B, which also requires INA-1/PAT-3 for invasive membrane localization (Fig. 7). The notion that integrin acts to coordinately regulate distinct signaling functions required for invasion is further supported by the synergistic genetic interactions between *ina-1* and *unc-40* shown previously (Hagedorn et al., 2009), as well *ina-1* and *mig-10*, and *unc-40* and *mig-10* demonstrated here. These genetic interaction studies suggest that there is a strong cooperative function between integrin, FOS-1A and netrin pathways during invasion.

How might integrin, netrin and FOS-1A function together to promote invasion? It has recently been shown that the invasive protrusion directed by UNC-40 enhances basement membrane gap opening by physically displacing matrix as the protrusion expands and extends through the basement membrane opening (Hagedorn et al., 2013). It is likely that FOS-1A transcriptional targets weaken the basement membrane by matrix remodeling, thus facilitating passage of the UNC-40-directed invasive protrusion. Thus, although each pathway has unique functions, successful invasion is dependent on both acting together. By localizing these pathways to the invasive cell membrane, integrin probably mediates the cooperative interactions between the FOS-1A targets and netrin effectors (and possibly other unidentified pathways). Together, these studies support the idea that integrin has a key scaffolding function within invasive cells that directs the trafficking or stabilization of distinct signaling molecules to the cell-basement membrane interface that act together to mediate the invasive process.

MATERIALS AND METHODS

Worm handling and strains

Worms were reared under standard conditions (Brenner, 1974). In the text and figures, we use a '>' symbol for linkages to a promoter and use a '::' symbol for linkages that fuse open reading frames. The following alleles and transgenes were used: *qyEx196 [unc-115 > GFP]*, *qyEx258 [unc-34 > GFP]*, *qyEx259 [cdh-3 > unc-40::GFP(overexpressed); myo-2 > GFP]*, *qyEx412 [cdh-3 > mig-10b(ΔN)::GFP; myo-2 > GFP]*, *qyIs28 [ced-10 > GFP::CED-10]*, *qyIs43 [pat-3::GFP; genomic ina-1]*, *qyIs57 [cdh-3 > mCherry::moeABD]*, *qyIs61 [cdh-3 > GFP::unc-34]*, *qyIs67 [cdh-3 > unc-40::GFP]*, *qyIs182 [cdh-3 > GFP::unc-115]*, *qyIs183 [cdh-3 > mig-*

Development (2014) doi:10.1242/dev.102434

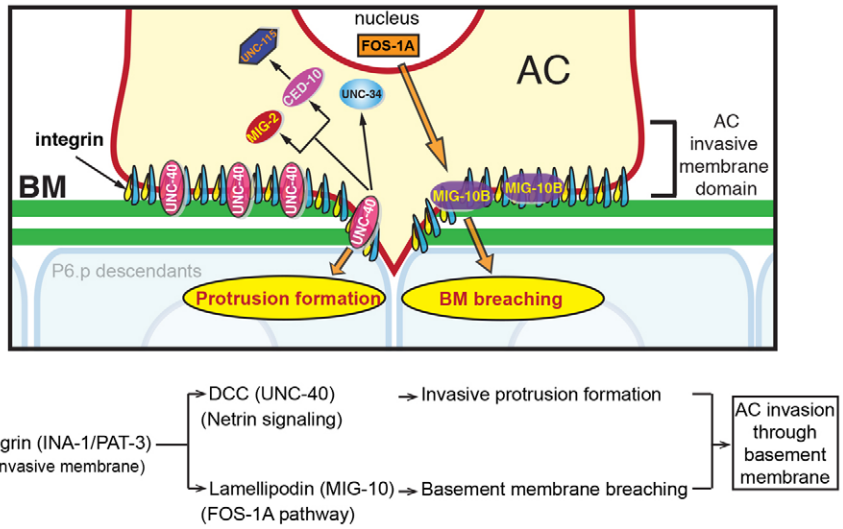

Fig. 7. Integrin localizes MIG-10B and DCC to the invasive cell membrane to coordinate basement membrane transmigration. UNC-6/UNC-40 (netrin), FOS-1A and INA-1/PAT-3 (integrin) function and localization during AC invasion. The INA-1/PAT-3 receptor has a scaffolding role at the invasive membrane, where it directs the trafficking or stabilization of both the netrin receptor UNC-40 and its effectors, which mediates invasive protrusion formation, and MIG-10B (lamellipodin), a target of FOS-1A, which promotes basement membrane breaching.

10b::GFP; cdh-3 > mChR], *qyIs220 [cdh-3 > GFP::mig-2]*, *qyIs221 [cdh-3 > GFP::ced-10]*, *sIs10246 [mig-10a > GFP]*, *sIs14214 [mig-10b > GFP]*, *olaEx889 [mig-10c > GFP]*; Linkage Group I (LGI): *unc-40(e271)*; LGII: *rrf-3(pk1426)*, *qyIs17 [zmp-1 > mCherry]*; LGIII: *ina-1(gm39)*, *mig-10(ct41)*, *mig-10(ok2499)*; LGIV: *ced-10(n1993)*, *qyIs10 [laminin::GFP]*, *qyIs15 [zmp-1 > HA- βtail]*; LGV: *unc-34(gm104)*, *unc-34(e951)*, *qyIs50 [cdh-3 > mCherry::moeABD]*; LGX: *unc-6(ev400)*, *unc-115(ky275)*, *mig-2(mu28)*, *him-4(rh319)*.

RNA interference

Double-strand RNA (dsRNA)-mediated gene interference (RNAi) was performed by feeding larvae with bacteria expressing dsRNA (Kamath et al., 2003). dsRNAi was targeted against *ced-10*, *ina-1* and *fos-1* to avoid larval lethality with genetic interactions, as well as sterility (Shakir et al., 2006; Sherwood et al., 2005). dsRNA targeting *ced-10* was delivered by feeding *mig-2(mu28)*, *unc-34(gm104),* or *unc-40(e271);mig-2(mu28)* to L4 larvae at 20°C; animals were allowed to grow to produce F1 progeny that were then analyzed. dsRNA targeting *ina-1* was delivered by feeding *rrf-3(pk1426)* and *rrf-3(pk1426);mig-10(ct41)* to L1 larvae. dsRNA targeting *fos-1* was delivered by feeding *qyEx196 [unc-115 >GFP]*, *qyEx258 [unc-34 >GFP]*, *qyIs28[ced-10 >GFP::CED-10]* and *qyIs43[pat-3::GFP; genomic ina-1]* to L1 larvae.

Scoring of AC invasion and polarity measurement

AC invasion was scored by examining the integrity of the phase-dense line between the AC and the descendants of the P6.p vulval precursor cell as previously described (Sherwood et al., 2005). Quantitative measurements of polarity were performed by determining the ratio of the average fluorescence intensity from a five-pixel-wide line drawn along the invasive (basal) versus the noninvasive (apical and lateral) membranes of images of the AC, using ImageJ software (Hagedorn et al., 2009).

Microscopy, image acquisition and processing, and quantitative analysis of F-actin and MIG-10

Images were acquired using a Zeiss AxioImager microscope with a 100× Plan-APOCHROMAT objective and equipped with a Yokogawa CSU-10 spinning disc confocal scan head controlled by iVision software (Biovision Technologies), or using a Zeiss AxioImager microscope with a 100× Plan-APOCHROMAT objective and a Zeiss AxioCam MRm CCD camera controlled by Axiovision software (Zeiss Microimaging). Acquired images were processed using ImageJ 1.40 and Photoshop CS3 Extended (Adobe Systems). Three-dimensional reconstructions were built from confocal *z*-stacks, analyzed and exported using Imaris 7.4 (Bitplane). F-actin and MIG-10 volume was measured using the 'isosurface rendering' function of Imaris (Hagedorn et al., 2009).

Quantitative analysis of suppression on UNC-40-overexpression phenotype

The ACs from animals overexpressing *cdh-3 > unc-40::GFP* in wild-type, *unc-34(gm104)*, *ced-10(n1993)* and *mig-2(mu28)* animals were imaged using 0.5 µm *z*-slice intervals on a confocal microscope. The *z*-stacks were then built into three-dimensional images. The number of protrusions on the apical and lateral membranes of ACs was determined and the length of protrusions was assessed using the Imaris measurement function.

Molecular biology and transgenic strains

Standard techniques were used to generate PCR fusion products (Hobert, 2002), plasmids and transgenic animals (Sherwood et al., 2005). Templates and specific PCR primers for promoters and genes, and transgenic extrachromosomal (Ex) lines and integrated strains (Is) generated in this study are listed in supplementary material Tables S1 and S2. To generate the transcriptional reporter for the *unc-115* gene, the promoter region 3.9 kb upstream of the ATG start codon of the *unc-115* gene was amplified. This promoter sequence was then fused in frame to the *GFP* coding sequence (vector pPD95.81) using PCR fusion. For the transcriptional reporter of the *unc-34* gene, 4.2 kb upstream of the *unc-34* coding sequence was PCR amplified and subcloned into pPD95.75 (GFP vector) at *Bam*HI and *Kpn*I sites. The *unc-115* cDNA amplified from N2 genomic DNA was PCR fused to the *cdh-3 >GFP* amplicon to generate *cdh-3 >GFP::unc-115*. AC-specific MIG-10B::GFP was generated by fusing the *cdh-3* promoter (Sherwood et al., 2005) to a coding sequence for MIG-10B::GFP amplified from the *unc-86 >mig-10b::GFP* vector (obtained from C. Bargmann, The Rockefeller University). To generate AC-specific *mig-10b(ΔN)::GFP*, *mig-10b(ΔN)::GFP* was amplified from the *unc-86 >mig-10b(ΔN)::GFP* vector and then fused to the *cdh-3* promoter. Transgenic worms were created by co-injection of expression constructs with the transformation marker pPD#MM016B (*unc-119+*), or the co-injection marker (*myo-2 >GFP*) or both into the germline of *unc-119(ed4)* mutants. These markers were injected with *Eco*RI-digested salmon sperm DNA and pBluescript II at 50 ng/µl as carrier DNA, along with the expression constructs, which were normally injected at 10-50 ng/µl. Integrated strains were generated as described previously (Sherwood et al., 2005).

Statistics

Statistical analysis was performed using Student's *t*-tests and Fisher's exact tests as indicated in the text.

Acknowledgements

We are grateful to E. A. Lundquist for the *unc-115(ky275) mig-2(mu28)* strain; the CGC for providing strains; D. A. Colon-Ramos for the *olaEx889[mig-10c >GFP]* strain; and C. I. Bargmann for the *unc-86 >mig-10b::GFP* plasmid.

Competing interests

The authors declare no competing financial interests.

Author contributions

D.R.S. and Z.W. analyzed and interpreted data, and wrote the manuscript. Experiments were designed by Z.W. and D.R.S. All experiments were performed by Z.W. with Q.C.'s assistance for the molecular cloning.

Funding

This work was supported by a Pew Scholars Award; and a National Institutes of Health grant [GM100083 to D.R.S.]. Deposited in PMC for release after 12 months.

Supplementary material

Supplementary material available online at
http://dev.biologists.org/lookup/suppl/doi:10.1242/dev.102434/-/DC1

References

Adler, C. E., Fetter, R. D. and Bargmann, C. I. (2006). UNC-6/Netrin induces neuronal asymmetry and defines the site of axon formation. *Nat. Neurosci.* **9**, 511-518.

Alexander, M., Chan, K. K., Byrne, A. B., Selman, G., Lee, T., Ono, J., Wong, E., Puckrin, R., Dixon, S. J. and Roy, P. J. (2009). An UNC-40 pathway directs postsynaptic membrane extension in Caenorhabditis elegans. *Development* **136**, 911-922.

Bader, B. L., Rayburn, H., Crowley, D. and Hynes, R. O. (1998). Extensive vasculogenesis, angiogenesis, and organogenesis precede lethality in mice lacking all alpha v integrins. *Cell* **95**, 507-519.

Baum, P. D. and Garriga, G. (1997). Neuronal migrations and axon fasciculation are disrupted in ina-1 integrin mutants. *Neuron* **19**, 51-62.

Bear, J. E. and Gertler, F. B. (2009). Ena/VASP: towards resolving a pointed controversy at the barbed end. *J. Cell Sci.* **122**, 1947-1953.

Brenner, S. (1974). The genetics of Caenorhabditis elegans. *Genetics* **77**, 71-94.

Brockbank, E. C., Bridges, J., Marshall, C. J. and Sahai, E. (2005). Integrin beta1 is required for the invasive behaviour but not proliferation of squamous cell carcinoma cells in vivo. *Br. J. Cancer* **92**, 102-112.

Burridge, K. and Wennerberg, K. (2004). Rho and Rac take center stage. *Cell* **116**, 167-179.

Caswell, P. T., Vadrevu, S. and Norman, J. C. (2009). Integrins: masters and slaves of endocytic transport. *Nat. Rev. Mol. Cell Biol.* **10**, 843-853.

Chang, C., Adler, C.E., Krause, M., Clark, S.G., Gertler, F.B., Tessier-Lavigne, M., and Bargmann, C.I. (2006). MIG-10/lamellipodin and AGE-1/PI3K promote axon guidance and outgrowth in response to slit and netrin. *Curr. Biol.* **16**, 854-862.

Coló, G. P., Lafuente, E. M. and Teixidó, J. (2012). The MRL proteins: adapting cell adhesion, migration and growth. *Eur. J. Cell Biol.* **91**, 861-868.

Colón-Ramos, D. A., Margeta, M. A. and Shen, K. (2007). Glia promote local synaptogenesis through UNC-6 (netrin) signaling in C. elegans. *Science* **318**, 103-106.

Demarco, R. S. and Lundquist, E. A. (2010). RACK-1 acts with Rac GTPase signaling and UNC-115/abLIM in Caenorhabditis elegans axon pathfinding and cell migration. *PLoS Genet.* **6**, e1001215.

Demarco, R. S., Struckhoff, E. C. and Lundquist, E. A. (2012). The Rac GTP exchange factor TIAM-1 acts with CDC-42 and the guidance receptor UNC-40/DCC in neuronal protrusion and axon guidance. *PLoS Genet.* **8**, e1002665.

Desgrosellier, J. S. and Cheresh, D. A. (2010). Integrins in cancer: biological implications and therapeutic opportunities. *Nat. Rev. Cancer* **10**, 9-22.

Dumartin, L., Quemener, C., Laklai, H., Herbert, J., Bicknell, R., Bousquet, C., Pyronnet, S., Castronovo, V., Schilling, M.K., Bikfalvi, A., et al. (2010). Netrin-1 mediates early events in pancreatic adenocarcinoma progression, acting on tumor and endothelial cells. *Gastroenterology* **138**, 1595-1606.e8.

Even-Ram, S. and Yamada, K. M. (2005). Cell migration in 3D matrix. *Curr. Opin. Cell Biol.* **17**, 524-532.

Felding-Habermann, B. (2003). Integrin adhesion receptors in tumor metastasis. *Clin. Exp. Metastasis* **20**, 203-213.

Gitai, Z., Yu, T. W., Lundquist, E. A., Tessier-Lavigne, M. and Bargmann, C. I. (2003). The netrin receptor UNC-40/DCC stimulates axon attraction and outgrowth through enabled and, in parallel, Rac and UNC-115/AbLIM. *Neuron* **37**, 53-65.

Guo, W. and Giancotti, F. G. (2004). Integrin signalling during tumour progression. *Nat. Rev. Mol. Cell Biol.* **5**, 816-826.

Hagedorn, E. J. and Sherwood, D. R. (2011). Cell invasion through basement membrane: the anchor cell breaches the barrier. *Curr. Opin. Cell Biol.* **23**, 589-596.

Hagedorn, E. J., Yashiro, H., Ziel, J. W., Ihara, S., Wang, Z. and Sherwood, D. R. (2009). Integrin acts upstream of netrin signaling to regulate formation of the anchor cell's invasive membrane in C. elegans. *Dev. Cell* **17**, 187-198.

Hagedorn, E. J., Ziel, J. W., Morrissey, M. A., Linden, L. M., Wang, Z., Chi, Q., Johnson, S. A. and Sherwood, D. R. (2013). The netrin receptor DCC focuses invadopodia-driven basement membrane transmigration in vivo. *J. Cell Biol.* **201**, 903-913.

Hedgecock, E. M., Culotti, J. G. and Hall, D. H. (1990). The unc-5, unc-6, and unc-40 genes guide circumferential migrations of pioneer axons and mesodermal cells on the epidermis in C. elegans. *Neuron* **4**, 61-85.

Hobert, O. (2002). PCR fusion-based approach to create reporter gene constructs for expression analysis in transgenic C. elegans. *Biotechniques* **32**, 728-730.

Hotary, K., Li, X. Y., Allen, E., Stevens, S. L. and Weiss, S. J. (2006). A cancer cell metalloprotease triad regulates the basement membrane transmigration program. *Genes Dev.* **20**, 2673-2686.

Hynes, R. O. (2012). The evolution of metazoan extracellular matrix. *J. Cell Biol.* **196**, 671-679.

Ihara, S., Hagedorn, E. J., Morrissey, M. A., Chi, Q., Motegi, F., Kramer, J. M. and Sherwood, D. R. (2011). Basement membrane sliding and targeted adhesion remodels tissue boundaries during uterine-vulval attachment in Caenorhabditis elegans. *Nat. Cell Biol.* **13**, 641-651.

Kalluri, R. (2003). Basement membranes: structure, assembly and role in tumour angiogenesis. *Nat. Rev. Cancer* **3**, 422-433.

Kamath, R. S., Fraser, A. G., Dong, Y., Poulin, G., Durbin, R., Gotta, M., Kanapin, A., Le Bot, N., Moreno, S., Sohrmann, M. et al. (2003). Systematic functional analysis of the Caenorhabditis elegans genome using RNAi. *Nature* **421**, 231-237.

Kaufmann, S., Kuphal, S., Schubert, T., and Bosserhoff, A.K. (2009). Functional implication of Netrin expression in malignant melanoma. *Cell. Oncol.* **31**, 415-422.

Kramer, J. M. (2005). Basement membranes. *WormBook* **2005**, 1-15.

Lafuente, E. M., van Puijenbroek, A. A., Krause, M., Carman, C. V., Freeman, G. J., Berezovskaya, A., Constantine, E., Springer, T. A., Gertler, F. B. and Boussiotis, V. A. (2004). RIAM, an Ena/VASP and Profilin ligand, interacts with Rap1-GTP and mediates Rap1-induced adhesion. *Dev. Cell* **7**, 585-595.

Lai Wing Sun, K., Correia, J. P. and Kennedy, T. E. (2011). Netrins: versatile extracellular cues with diverse functions. *Development* **138**, 2153-2169.

Lambert, E., Coissieux, M. M., Laudet, V. and Mehlen, P. (2012). Netrin-4 acts as a pro-angiogenic factor during zebrafish development. *J. Biol. Chem.* **287**, 3987-3999.

Lebrand, C., Dent, E. W., Strasser, G. A., Lanier, L. M., Krause, M., Svitkina, T. M., Borisy, G. G. and Gertler, F. B. (2004). Critical role of Ena/VASP proteins for filopodia formation in neurons and in function downstream of netrin-1. *Neuron* **42**, 37-49.

Lee, M., Cram, E. J., Shen, B. and Schwarzbauer, J. E. (2001). Roles for beta(pat-3) integrins in development and function of Caenorhabditis elegans muscles and gonads. *J. Biol. Chem.* **276**, 36404-36410.

Lee, H.-S., Lim, C. J., Puzon-McLaughlin, W., Shattil, S. J. and Ginsberg, M. H. (2009). RIAM activates integrins by linking talin to ras GTPase membrane-targeting sequences. *J. Biol. Chem.* **284**, 5119-5127.

Legate, K. R., Wickström, S. A. and Fässler, R. (2009). Genetic and cell biological analysis of integrin outside-in signaling. *Genes Dev.* **23**, 397-418.

Leptin, M., Bogaert, T., Lehmann, R. and Wilcox, M. (1989). The function of PS integrins during Drosophila embryogenesis. *Cell* **56**, 401-408.

Li, X., Meriane, M., Triki, I., Shekarabi, M., Kennedy, T. E., Larose, L. and Lamarche-Vane, N. (2002a). The adaptor protein Nck-1 couples the netrin-1 receptor DCC (deleted in colorectal cancer) to the activation of the small GTPase Rac1 through an atypical mechanism. *J. Biol. Chem.* **277**, 37788-37797.

Li, X., Saint-Cyr-Proulx, E., Aktories, K. and Lamarche-Vane, N. (2002b). Rac1 and Cdc42 but not RhoA or Rho kinase activities are required for neurite outgrowth induced by the Netrin-1 receptor DCC (deleted in colorectal cancer) in N1E-115 neuroblastoma cells. *J. Biol. Chem.* **277**, 15207-15214.

Lundquist, E. A., Herman, R. K., Shaw, J. E. and Bargmann, C. I. (1998). UNC-115, a conserved protein with predicted LIM and actin-binding domains, mediates axon guidance in C. elegans. *Neuron* **21**, 385-392.

Luo, Y. P., Zhou, H., Krueger, J., Kaplan, C., Liao, D., Markowitz, D., Liu, C., Chen, T., Chuang, T. H., Xiang, R. et al. (2010). The role of proto-oncogene Fra-1 in remodeling the tumor microenvironment in support of breast tumor cell invasion and progression. *Oncogene* **29**, 662-673.

Machesky, L., Jurdic, P. and Hinz, B. (2008). Grab, stick, pull and digest: the functional diversity of actin-associated matrix-adhesion structures. Workshop on invadopodia, podosomes and focal adhesions in tissue invasion. *EMBO Rep.* **9**, 139-143.

Manser, J. and Wood, W. B. (1990). Mutations affecting embryonic cell migrations in Caenorhabditis elegans. *Dev. Genet.* **11**, 49-64.

Manser, J., Roonprapunt, C. and Margolis, B. (1997). C. elegans cell migration gene mig-10 shares similarities with a family of SH2 domain proteins and acts cell nonautonomously in excretory canal development. *Dev. Biol.* **184**, 150-164.

Marlin, S. D., Morton, C. C., Anderson, D. C. and Springer, T. A. (1986). LFA-1 immunodeficiency disease. Definition of the genetic defect and chromosomal mapping of alpha and beta subunits of the lymphocyte function-associated antigen 1 (LFA-1) by complementation in hybrid cells. *J. Exp. Med.* **164**, 855-867.

Matus, D. Q., Li, X. Y., Durbin, S., Agarwal, D., Chi, Q., Weiss, S. J. and Sherwood, D. R. (2010). In vivo identification of regulators of cell invasion across basement membranes. *Sci. Signal.* **3**, ra35.

Milde-Langosch, K. (2005). The Fos family of transcription factors and their role in tumourigenesis. *Eur. J. Cancer* **41**, 2449-2461.

Nguyen, A. and Cai, H. (2006). Netrin-1 induces angiogenesis via a DCC-dependent ERK1/2-eNOS feed-forward mechanism. *Proc. Natl. Acad. Sci. USA* **103**, 6530-6535.

Nourshargh, S., Hordijk, P. L. and Sixt, M. (2010). Breaching multiple barriers: leukocyte motility through venular walls and the interstitium. *Nat. Rev. Mol. Cell Biol.* **11**, 366-378.

Ozanne, B. W., Spence, H. J., McGarry, L. C. and Hennigan, R. F. (2007). Transcription factors control invasion: AP-1 the first among equals. *Oncogene* **26**, 1-10.

Pérez-Pérez, J. M., Candela, H. and Micol, J. L. (2009). Understanding synergy in genetic interactions. *Trends Genet.* **25**, 368-376.

Quinn, C. C., Pfeil, D. S., Chen, E., Stovall, E. L., Harden, M. V., Gavin, M. K., Forrester, W. C., Ryder, E. F., Soto, M. C. and Wadsworth, W. G. (2006). UNC-6/netrin and SLT-1/slit guidance cues orient axon outgrowth mediated by MIG-10/RIAM/lamellipodin. *Curr. Biol.* **16**, 845-853.

Quinn, C. C., Pfeil, D. S., and Wadsworth, W. G. (2008). CED-10/Rac1 mediates axon guidance by regulating the asymmetric distribution of MIG-10/lamellipodin. *Curr. Biol.* **18**, 808-813.

Reddien, P. W. and Horvitz, H. R. (2000). CED-2/CrkII and CED-10/Rac control phagocytosis and cell migration in Caenorhabditis elegans. *Nat. Cell Biol.* **2**, 131-136.
Rowe, R. G. and Weiss, S. J. (2008). Breaching the basement membrane: who, when and how? *Trends Cell Biol.* **18**, 560-574.
Shakir, M. A., Gill, J. S. and Lundquist, E. A. (2006). Interactions of UNC-34 Enabled with Rac GTPases and the NIK kinase MIG-15 in Caenorhabditis elegans axon pathfinding and neuronal migration. *Genetics* **172**, 893-913.
Shakir, M. A., Jiang, K., Struckhoff, E. C., Demarco, R. S., Patel, F. B., Soto, M. C. and Lundquist, E. A. (2008). The Arp2/3 activators WAVE and WASP have distinct genetic interactions with Rac GTPases in Caenorhabditis elegans axon guidance. *Genetics* **179**, 1957-1971.
Sharma-Kishore, R., White, J. G., Southgate, E. and Podbilewicz, B. (1999). Formation of the vulva in Caenorhabditis elegans: a paradigm for organogenesis. *Development* **126**, 691-699.
Shekarabi, M. and Kennedy, T. E. (2002). The netrin-1 receptor DCC promotes filopodia formation and cell spreading by activating Cdc42 and Rac1. *Mol. Cell. Neurosci.* **19**, 1-17.
Shekarabi, M., Moore, S. W., Tritsch, N. X., Morris, S. J., Bouchard, J. F. and Kennedy, T. E. (2005). Deleted in colorectal cancer binding netrin-1 mediates cell substrate adhesion and recruits Cdc42, Rac1, Pak1, and N-WASP into an intracellular signaling complex that promotes growth cone expansion. *J. Neurosci.* **25**, 3132-3141.
Sherwood, D. R. and Sternberg, P. W. (2003). Anchor cell invasion into the vulval epithelium in C. elegans. *Dev. Cell* **5**, 21-31.
Sherwood, D. R., Butler, J. A., Kramer, J. M. and Sternberg, P. W. (2005). FOS-1 promotes basement-membrane removal during anchor-cell invasion in C. elegans. *Cell* **121**, 951-962.
Sixt, M., Bauer, M., Lämmermann, T. and Fässler, R. (2006). Beta1 integrins: zip codes and signaling relay for blood cells. *Curr. Opin. Cell Biol.* **18**, 482-490.
Stavoe, A. K. and Colón-Ramos, D. A. (2012). Netrin instructs synaptic vesicle clustering through Rac GTPase, MIG-10, and the actin cytoskeleton. *J. Cell Biol.* **197**, 75-88.
Stavoe, A. K., Nelson, J. C., Martínez-Velázquez, L. A., Klein, M., Samuel, A. D. and Colón-Ramos, D. A. (2012). Synaptic vesicle clustering requires a distinct MIG-10/Lamellipodin isoform and ABI-1 downstream from Netrin. *Genes Dev.* **26**, 2206-2221.
Struckhoff, E. C. and Lundquist, E. A. (2003). The actin-binding protein UNC-115 is an effector of Rac signaling during axon pathfinding in C. elegans. *Development* **130**, 693-704.
Teichmann, H. M. and Shen, K. (2011). UNC-6 and UNC-40 promote dendritic growth through PAR-4 in Caenorhabditis elegans neurons. *Nat. Neurosci.* **14**, 165-172.
Uhlirova, M. and Bohmann, D. (2006). JNK- and Fos-regulated Mmp1 expression cooperates with Ras to induce invasive tumors in Drosophila. *EMBO J.* **25**, 5294-5304.
Wang, Z. and Sherwood, D. R. (2011). Chapter 5 – Dissection of genetic pathways in C. elegans. In *Methods in Cell Biology* (ed. J. H. Rothman and A. Singson), pp. 113-157. Waltham, MA: Academic Press.
Wang, S., Voisin, M. B., Larbi, K. Y., Dangerfield, J., Scheiermann, C., Tran, M., Maxwell, P. H., Sorokin, L. and Nourshargh, S. (2006). Venular basement membranes contain specific matrix protein low expression regions that act as exit points for emigrating neutrophils. *J. Exp. Med.* **203**, 1519-1532.
Withee, J., Galligan, B., Hawkins, N. and Garriga, G. (2004). Caenorhabditis elegans WASP and Ena/VASP proteins play compensatory roles in morphogenesis and neuronal cell migration. *Genetics* **167**, 1165-1176.
Young, M. R. and Colburn, N. H. (2006). Fra-1 a target for cancer prevention or intervention. *Gene* **379**, 1-11.
Yu, T. W., Hao, J. C., Lim, W., Tessier-Lavigne, M. and Bargmann, C. I. (2002). Shared receptors in axon guidance: SAX-3/Robo signals via UNC-34/Enabled and a Netrin-independent UNC-40/DCC function. *Nat. Neurosci.* **5**, 1147-1154.
Ziel, J. W., Hagedorn, E. J., Audhya, A. and Sherwood, D. R. (2009). UNC-6 (netrin) orients the invasive membrane of the anchor cell in C. elegans. *Nat. Cell Biol.* **11**, 183-189.
Zipkin, I. D., Kindt, R. M. and Kenyon, C. J. (1997). Role of a new Rho family member in cell migration and axon guidance in C. elegans. *Cell* **90**, 883-894.

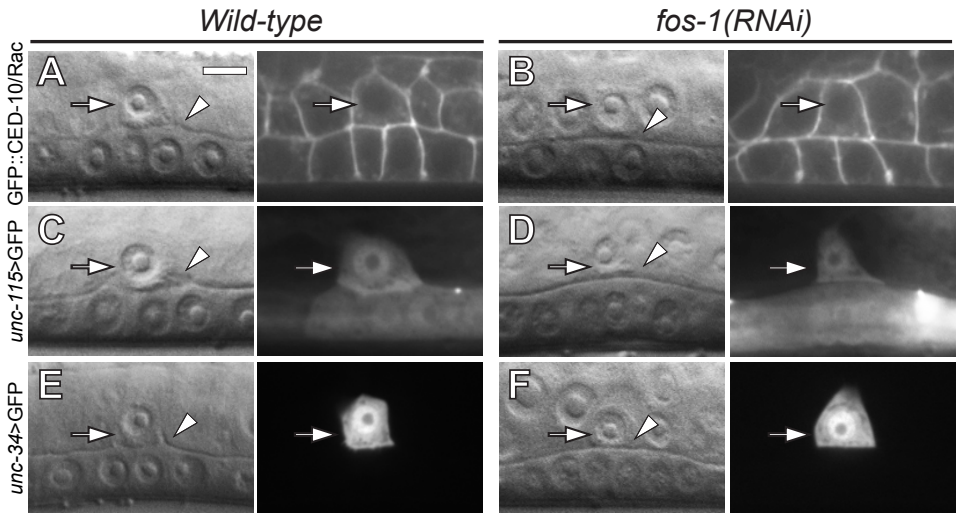

Fig. S1. FOS-1A does not regulate the expression of UNC-40 effectors.
DIC images (left) and corresponding fluorescence images (right) are shown at the P6.p four-cell stage. (A) GFP::CED-10 driven by its endogenous promoter is expressed and was localized to the membrane of the wild-type AC. (B) The expression and localization of CED-10 was unaffected (arrow) after *fos-1* RNAi treatment, which blocked AC invasion (arrowhead denotes intact phase dense line representing basement membrane). (C and E) The transcriptional reporters for *unc-115* (*unc-115 > GFP*) and *unc-34* (*unc-34 > GFP*) showed AC expression. (D and F) The expression of transcriptional reporters for *unc-115* and *unc-34* remained unchanged after *fos-1* RNAi treatment. In this and all other supplementary figures, scale bars represent 5 μm.

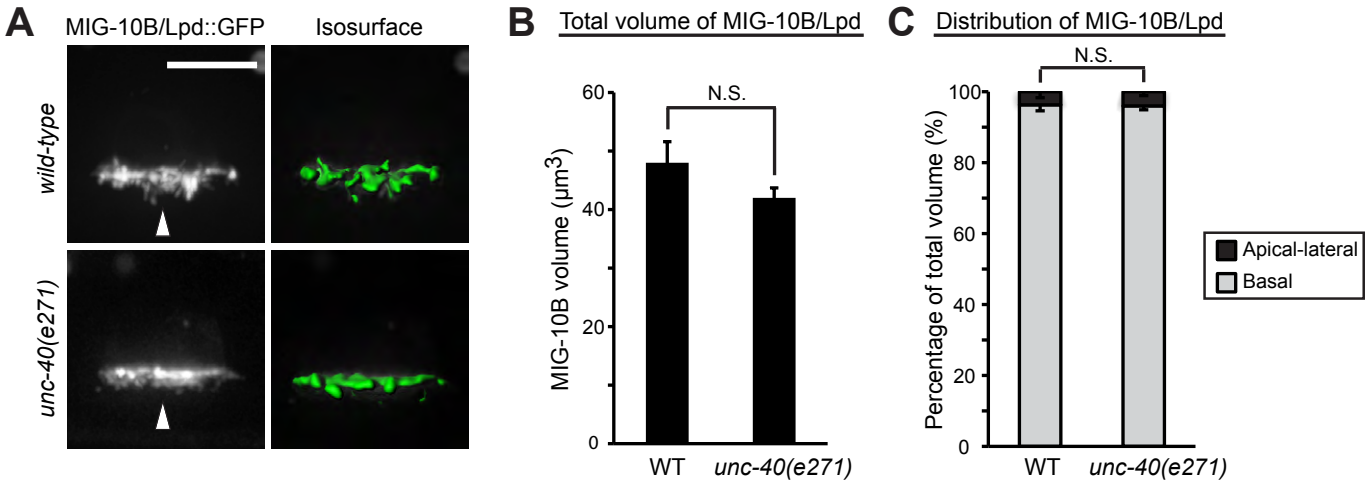

Fig. S2. MIG-10B localization remains polarized in *unc-40(e271)* mutant ACs.
(A) Images show 3D reconstructions generated from confocal z-stacks taken in animals at the P6.p four-cell stage. Fluorescence (left) and corresponding isosurface rendering of MIG-10B::GFP localization (right). MIG-10B polarizes to the invasive cell membrane (white arrowheads) in wild-type ACs and *unc-40* mutant ACs at the P6.p four-cell stage. (B) Quantification of the total MIG-10B volume in wild-type and *unc-40(e271)* mutant ACs at the P6.p four-cell stage (n ≥ 10 per genotype). (C) The basal (gray) and apical-lateral (black) distribution of MIG-10B within the AC in wild-type animals and *unc-40(e271)* mutants at the P6.p four-cell stage (n ≥ 10 per genotype). In this and all other supplementary figures, one asterisk (*), two asterisks (**) and three asterisks (***) indicate statistically-significant differences of $P < 0.05$, $P < 0.01$ and $P < 0.001$, respectively, and N.S. indicates no significant difference (Student's *t*-test). Error bars represent the standard error of the mean. Significant differences relative to wild-type animals are indicated.

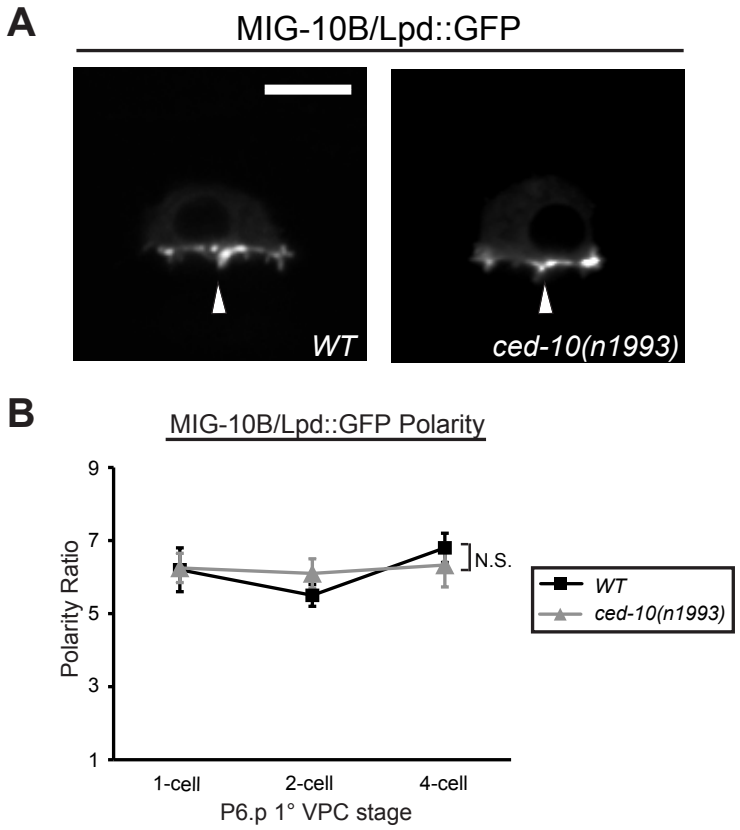

Fig. S3. MIG-10B localization remains polarized in *ced-10(n1993)* mutant ACs.
(A) MIG-10B polarizes to the invasive cell membrane (white arrowheads) in wild-type ACs and *ced-10* mutant ACs at the P6.p four-cell stage. (B) Quantification of MIG-10B polarization to the invasive cell membrane in wild-type animals (black squares), *unc-40* mutants (gray triangles) at the P6.p one-, two-, and four-cell stages (n ≥ 12 for each stage per genotype). Significant differences relative to wild-type animals are indicated.

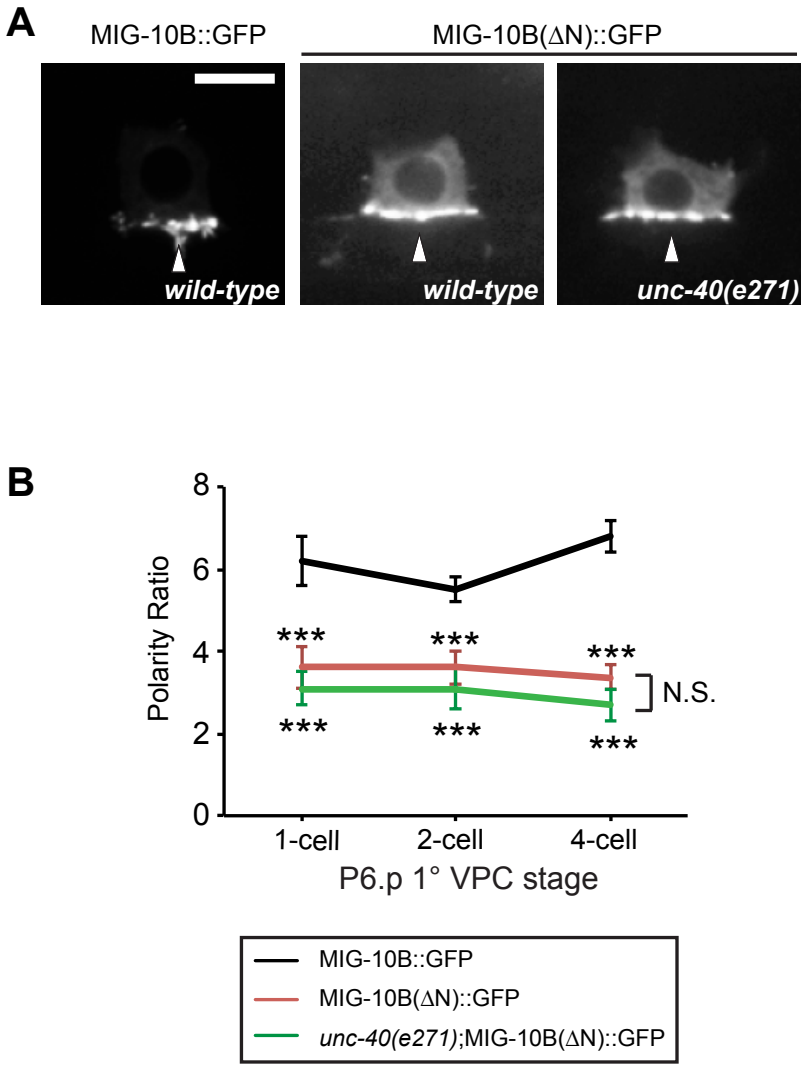

Fig. S4. The N-terminal domain of MIG-10B promotes localization to the invasive membrane.
(A) In wild-type ACs, MIG-10B was strongly polarized to the invasive cell membrane (white arrowhead). MIG-10B(ΔN) showed reduced localization to the invasive cell membrane (white arrowhead), which was not further reduced in *unc-40* mutants. (B) Quantification of polarization of MIG-10B in wild-type animals (black line) and MIG-10B(ΔN) in wild-type (red line) and *unc-40* (green line) mutant animals at the P6.p one-, two-, and four-cell stages ($n \geq 12$ for each stage per genotype). Significant differences relative to wild-type animals are indicated.

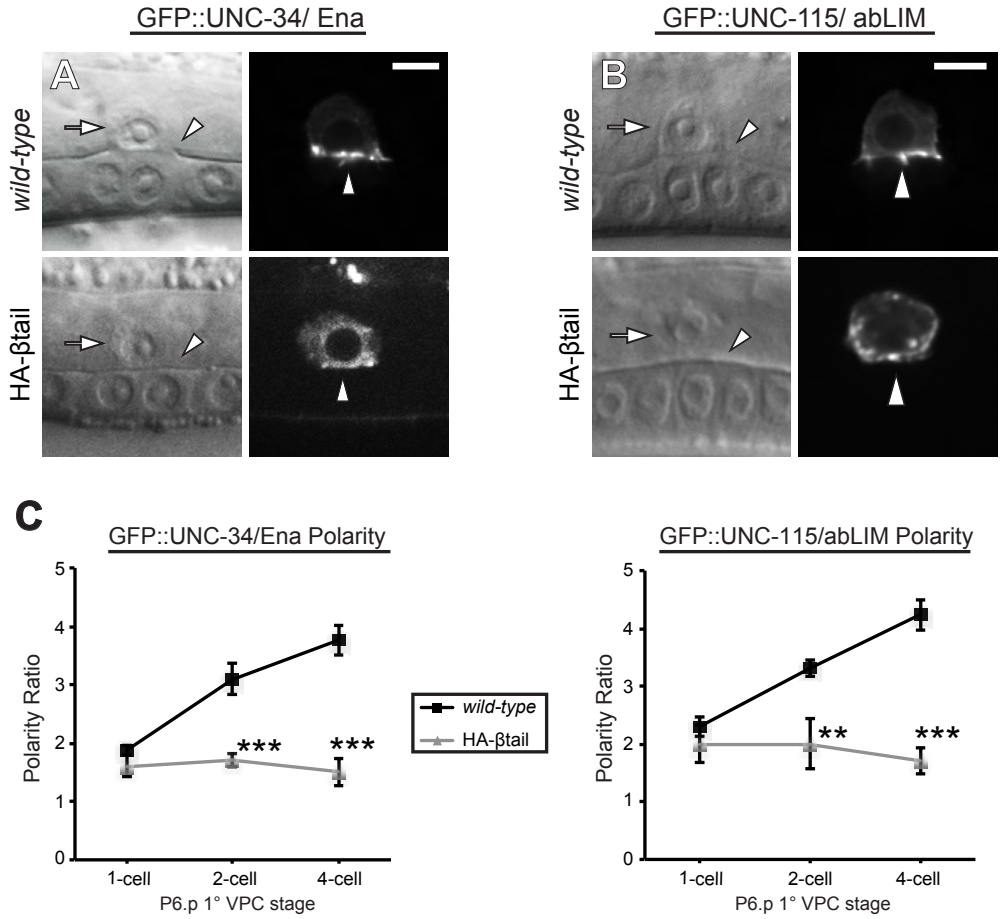

Fig. S5. Integrin localizes UNC-34 and UNC-115 to the invasive cell membrane.
(A and B) DIC images (left) and corresponding fluorescence (right). In wild-type ACs, UNC-34 and UNC-115 polarized to the invasive cell membrane (white arrowheads). In contrast, expression of a dominant negative integrin PAT-3 β subunit in the AC (*zmp-1 > HA- βtail*) reduced the polarization of UNC-34 and UNC-115 to the invasive membrane. ACs in *HA- βtail* animals still adhered to the underlying basement membrane (arrowhead, DIC image). (C) Quantification of UNC-34 and UNC-115 polarization to the invasive cell membrane in wild-type animals (black squares) and HA- βtail (gray triangles) at the P6.p one-, two-, and four-cell stages ($n \geq 12$ for each stage per genotype). Significant differences relative to wild-type animals are indicated.

Table S1. Primer sequences and templates used for PCR fusions and cloning

Primer sequence (5'->3')	Primer type	Amplicon	Template
TAATGTGAGTTAGCTCACT CATTAGG	Forward	*cdh-3 promoter*	pPD107.94/mk62 -63
AACGATGGATACGCTAACA ACTTGG	Forward nested	*cdh-3 promoter*	pPD107.94/mk62 -63
TTTCTGAGCTCGGTACCCTC CAAG	Reverse	*cdh-3 promoter*	pPD107.94/mk62 -63
ATGAGTAAAGGAGAAGAA CTTTTCAC	Forward	*GFP*	pPD95.81 (GFP)
GGAAACAGTTATGTTTGGT ATATTGGG	Reverse nested	*GFP*	pPD95.81 (GFP); Plasmid *unc-86 > mig-10::GFP*
AAGGGCCCGTACGGCCGAC TA	Reverse	*GFP*	pPD95.81 (GFP); Plasmid *unc-86 > mig-10::GFP*
TTTGTATAGTTCATCCATGC CATGTG	Reverse for GFP extension to N-terminus of protein of interest	*GFP*	Plasmid *cdh-3 > GFP*
GTGCCCGTAAATCAATACC TAGTC	Forward	*unc-34 promoter*	N2 genomic DNA
GCACTTTTACGGCAGATTTT GTGT	Reverse	*unc-34 promoter*	N2 genomic DNA
GCTCATCCCTGATTACAAG TTT	Forward	*unc-115 promoter for unc-115 > GFP*	N2 genomic DNA
CGAAGCACGGAATAAATCA T	Forward nested	*unc-115 promoter for unc-115 > GFP*	N2 genomic DNA
GGTATAGAATAGCGGAGAG AGGTCT	Reverse	*unc-115 promoter for unc-115 > GFP*	N2 genomic DNA
GACCTCTCTCCGCTATTCTA TACCATGAGTAAAGGAGAA GAACTTTT	Forward GFP extension	*GFP for unc-115 > GFP*	pPD95.81 (GFP)
ATGGGCAAAAAATGCGACG TATGT	Forward	*unc-115 cDNA for cdh-3 > GFP::unc-115*	N2 cDNA
GACTTGGAGACAAATAACG GGGAT	Reverse	*unc-115 cDNA for cdh-3 > GFP::unc-115*	N2 cDNA
CGAGATTCCGCGTAGAAGA CAAA	Reverse nested	*unc-115 cDNA for cdh-3 > GFP::unc-115*	N2 cDNA
CATACGTCGCATTTTTTGCC CATTTTGTATAGTTCATCCA TGCCA	Reverse for GFP with *unc-115* extension	*GFP for cdh-3 > GFP::unc-115*	Plasmid *cdh-3 > GFP*
CTTGGAGGGTACCGAGCTC AGAAAATGTATCACGATCG ACGG	Forward *cdh-3* promoter extension	*mig-10b::GFP for cdh-3 > mig-10b::GFP*	Plasmid *unc-86 > mig-10::GFP*
CTTGGAGGGTACCGAGCTC AGAAAATGTCCGCAGATTG GCAGTTG	Forward *cdh-3* promoter extension	*mig-10b(ΔN)::GFP for cdh-3 > mig-10b(ΔN)::GFP*	Plasmid *unc-86 > mig-10::GFP*

Table S2. Extrachromosomal array and integrated strain generation

Strain Designation	PCR fusion or plamids	Injection concentration (ng/µl)	Co-injection marker
qyEx196	*unc-115 > GFP* [a]	50	*unc-119+*
qyEx258	*unc-34 > GFP* [b]	50	*unc-119+*
qyEx259 (overexpression)	*cdh-3 > unc-40::GFP* [a]	50	*unc-119+, myo-2 > GFP*
qyEx412	*cdh-3 > mig-10b(ΔN)::GFP* [a]	10	*unc-119+, myo-2 > GFP*
qyIs182	*cdh-3 > GFP::unc-115* [a]	50	*unc-119+*
qyIs183	*cdh-3 > mig-10b::GFP* [a]	10	*unc-119+*

[a] PCR fusion product; [b] plasmid